

*Annual Review of Plant Biology***Adaptable and Multifunctional  
Ion-Conducting Aquaporins****Stephen D. Tyerman,<sup>1</sup> Samantha A. McGaughey,<sup>2</sup>  
Jiaen Qiu,<sup>1</sup> Andrea J. Yool,<sup>3</sup> and Caitlin S. Byrt<sup>2</sup>**

<sup>1</sup>Australian Research Council (ARC) Centre of Excellence in Plant Energy Biology, School of Agriculture, Food and Wine, University of Adelaide, Glen Osmond, South Australia 5064, Australia; email: [steve.tyerman@adelaide.edu.au](mailto:steve.tyerman@adelaide.edu.au), [Jiaen.Qiu@adelaide.edu.au](mailto:Jiaen.Qiu@adelaide.edu.au)

<sup>2</sup>ARC Centre of Excellence for Translational Photosynthesis, Division of Plant Sciences, Research School of Biology, Australian National University, Acton, Australian Capital Territory 0200, Australia; email: [Samantha.McGaughey@anu.edu.au](mailto:Samantha.McGaughey@anu.edu.au), [Caitlin.Byrt@anu.edu.au](mailto:Caitlin.Byrt@anu.edu.au)

<sup>3</sup>Adelaide Medical School, University of Adelaide, Adelaide, South Australia 5005, Australia; email: [andrea.yool@adelaide.edu.au](mailto:andrea.yool@adelaide.edu.au)

Annu. Rev. Plant Biol. 2021. 72:703–36

First published as a Review in Advance on  
February 12, 2021

The *Annual Review of Plant Biology* is online at  
[plant.annualreviews.org](http://plant.annualreviews.org)

<https://doi.org/10.1146/annurev-arplant-081720-013608>

Copyright © 2021 by Annual Reviews.  
All rights reserved

**Keywords**

nonselective cation channel, anion channel, electroosmosis, water pumping, ion channel, channel gating

**Abstract**

Aquaporins function as water and neutral solute channels, signaling hubs, disease virulence factors, and metabolon components. We consider plant aquaporins that transport ions compared to some animal counterparts. These are candidates for important, as yet unidentified, cation and anion channels in plasma, tonoplast, and symbiotic membranes. For those individual isoforms that transport ions, water, and gases, the permeability spans 12 orders of magnitude. This requires tight regulation of selectivity via protein interactions and postranslational modifications. A phosphorylation-dependent switch between ion and water permeation in AtPIP2;1 might be explained by coupling between the gates of the four monomer water channels and the central pore of the tetramer. We consider the potential for coupling between ion and water fluxes that could form the basis of an electroosmotic transducer. A grand challenge in understanding the roles of ion transporting aquaporins is their multifunctional modes that are dependent on location, stress, time, and development.

**ANNUAL  
REVIEWS CONNECT**

[www.annualreviews.org](http://www.annualreviews.org)

- Download figures
- Navigate cited references
- Keyword search
- Explore related articles
- Share via email or social media

## Contents

INTRODUCTION .....	704
Functional Insights from Structural Comparisons of Aquaporins .....	706
The Challenge of Multiple Transport Substrates and Diverse Roles .....	707
PLANT ION-CONDUCTING AQUAPORINS .....	708
Tonoplast Intrinsic Proteins .....	708
NOD26: A NIP for N <sub>2</sub> -Fixing Symbiosis .....	710
VvXIP1 Facilitates Copper and Nickel Transport .....	712
OsPIP1;3: A Multifunctional Water and Anion Channel? .....	712
The Cation-Conducting AtPIP2;1, AtPIP2;2, and HvPIP2;8 .....	715
Can PIP2 Structure Be Reconciled with Ion Transport? The AQP1 Parallel .....	719
AtPIP2;1: A Multifunctional Conditional System with a Large Permissive Permeability Range .....	723
FUTURE PERSPECTIVES ON THE DISCOVERY OF PLANT ION-CONDUCTING AQUAPORINS AND THEIR ROLES .....	724

## INTRODUCTION

Aquaporins (AQPs), known for facilitating passive water permeation across membranes, belong to an extensive and ancient family of major intrinsic proteins (MIPs). We use the term aquaporin for members of the MIP family, with the caveat that some do not function as water channels and many others transport more than water. Nomenclature introduced to indicate specific solute permeabilities includes peroxiporins (H<sub>2</sub>O<sub>2</sub>), aquaglyceroporins (glycerol and urea), metalloiodoporins (boron, silicon, selenium, and others), gas channels (CO<sub>2</sub> and O<sub>2</sub>), and aquaammoniaporins (NH<sub>3</sub>). Other reviews detail the different roles of diverse classes of AQPs (20, 46, 107, 130, 201). In addition to facilitating permeation of small neutral solutes and/or water, some AQPs also facilitate electrogenic transport of cations or anions, serving as ion-conducting AQPs (icaAQPs), which are distinct from those that may transport an ion as a neutral complex (208). icaAQPs are an emerging area of interest in the AQP field that may reframe our understanding of transport biology. This review examines the evidence for plant icaAQPs and compares their mechanisms with those of established animal icaAQPs.

Based on sequence similarities, plant kingdom AQPs are classified into some 13 subfamilies (42, 107), of which 5 occur in higher plants; evolutionary relationships and proposed origins of subfamilies have been addressed in detail elsewhere (2, 20, 25, 147). Subfamilies can be further divided based on selectivity for neutral solutes (2, 203), but selectivity and membrane location can overlap to various degrees, and icaAQPs are indicated (some putatively) in four of the five subfamilies in seed plants [nodulin-26-like intrinsic proteins (NIPs), tonoplast intrinsic proteins (TIPs), plasma membrane intrinsic proteins (PIPs), and X intrinsic proteins (XIPs), but not small basic intrinsic proteins (SIPs)] thus far (**Figure 1**). Not enough detail is yet available to indicate specific ionic selectivity differences of icaAQPs between subfamilies. The icaAQPs have been demonstrated in heterologous expression systems or by incorporation of purified protein into membrane bilayers, the same methods that have been relied upon to designate water and neutral solute permeation of AQPs. The putative icaAQP isoforms considered in detail here are TaTIP2;1 (77), GmNOD26 (the archetypal soybean NIP) (54, 87, 210), VvXIP1 (137), OsPIP1;3 (119, 123), AtPIP2;1 (PIP2A) and AtPIP2;2 (PIP2B) (32, 94, 101), and HvPIP2;8 (190), and in addition some examples of orthologs that show unorthodox multifunctional roles (**Figure 1**). However, when assigning ion transport

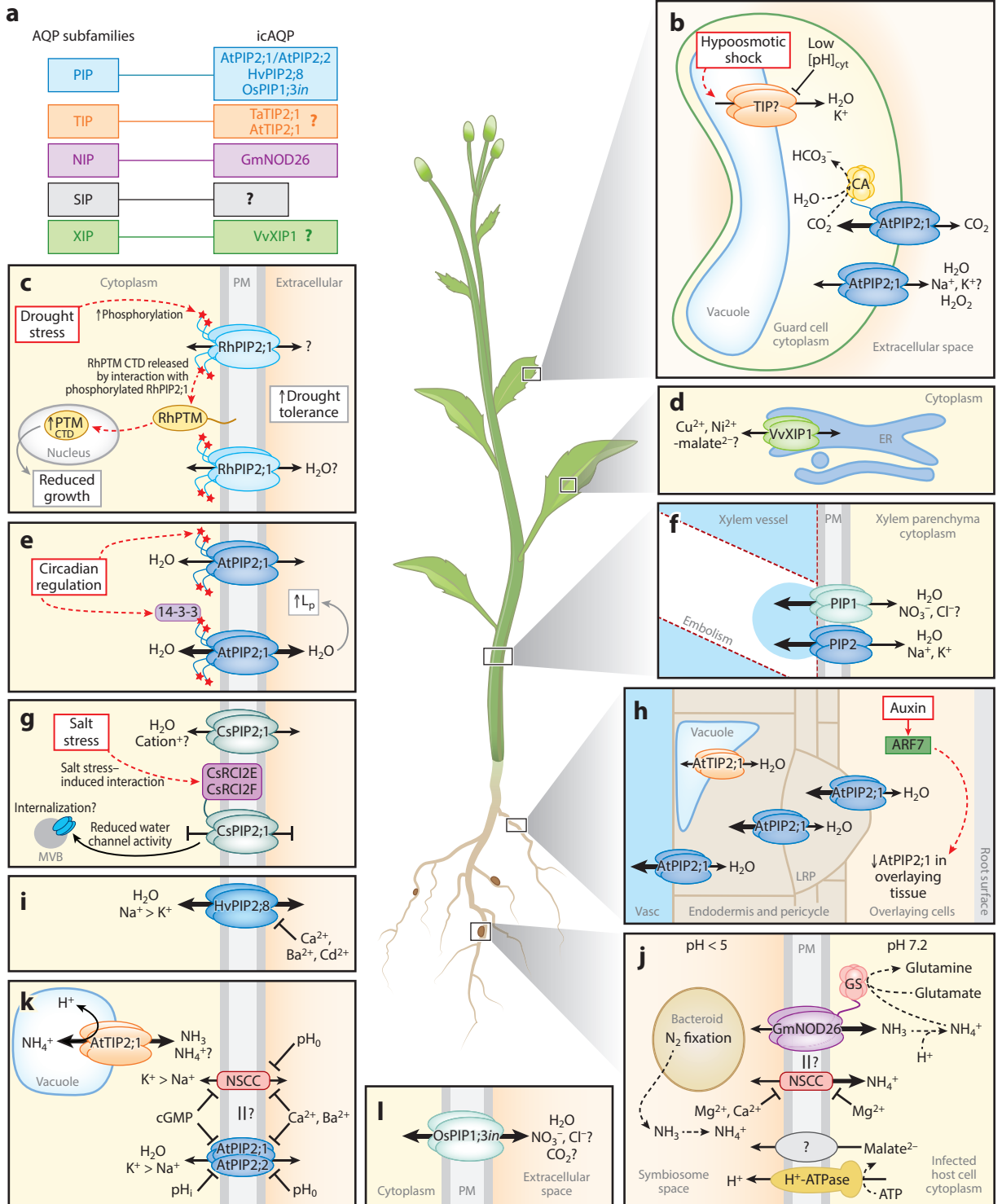
---

**Electrogenic:** a net flux of ions across a membrane resulting in a change in membrane voltage (i.e., transmembrane potential difference)

**Heterologous expression:** expression of a protein experimentally induced in a cell that does not normally make that protein

**Isoform:** functionally similar proteins that have similar but not identical amino acid sequences

---



(Caption appears on following page)

## Figure 1 (Figure appears on preceding page)

The diverse roles of multifunctional (putative) icAQPs. (a) Plant AQPs are classified into five subfamilies: PIPs (PIP1 and PIP2), TIPs (5 groups), NIPs (7 groups), SIPs (2 groups), and the uncharacterized XIPs (4 groups). icAQPs have been identified by functional assays in the PIP (32, 123, 190) and NIP (210) subfamilies and suggested for the TIP (77) and XIP (137) subfamilies. (b) Guard cell TIP and AtPIP2;1 are implicated in stomatal closure (66, 167, 205). (c) Rose RhPIP2;1 may act as a drought sensor interacting with a membrane-tethered (putative) transcription factor RhPTM (236). (d) Grape VvXIP1 on the ER in leaves may transport  $\text{Cu}^{2+}$  and  $\text{Ni}^{2+}$  ions (137) or uncharged complexes (208). (e) Diurnal regulation of *Arabidopsis* rosette hydraulic conductivity is proposed to occur via interaction between 14-3-3 proteins and C-terminal phosphorylated AtPIP2;1 (152). (f) icAQPs may have a role in xylem embolism repair (171, 180). (g) *Camelina sativa* CsPIP2;1 water transport is regulated by interaction with Rare Cold Inducible proteins under salinity stress (97). (h) *Arabidopsis* lateral root emergence is regulated by AtPIP2;1 (146) and AtTIP2;1 (163). (i) Barley HvPIP2;8 expressed in leaves and roots transports  $\text{H}_2\text{O}$ ,  $\text{Na}^+$ , and  $\text{K}^+$ ; is inhibited by divalents; and is linked to salt tolerance (190). (j) Soybean GmNOD26 is a candidate  $\text{NH}_4^+$ -NSCC on the SM of N-fixing nodules (128, 193). (k) *Arabidopsis* AtPIP2;1 and AtPIP2;2 are candidates for the vi-NSCCs (32, 101) observed in the patch clamp of root protoplasts (44). AtTIP2;1 as an  $\text{NH}_4^+$ -trapping mechanism in vacuoles (124). (l) Rice OsPIP1;3*in* transports water and  $\text{NO}_3^-$  (123). See **Supplemental Table 1** for summary and additional details. Symbols and arrows: solid black arrows, transport directions (size indicates relative amount of transport); dashed black arrows, enzymic or chemical reactions; blunt solid black arrows, inhibition; dashed red arrows, signals; solid gray arrows, proposed physiological effect; red star, phosphorylation. Abbreviations: AQP, aquaporin; ATP, adenosine triphosphate; CA, carbonic anhydrase; cGMP, guanosine 3',5'-cyclic monophosphate; CTD, C-terminal domain; ER, endoplasmic reticulum; GS, glutamine synthetase; icAQP, ion-conducting aquaporin;  $L_p$ , hydraulic conductance of rosette; LRP, lateral root primordium; MVB, multivesicular bodies; NSCC, nonselective cation channel; NIP, nodulin-26-like protein; PIP, plasma membrane intrinsic protein; PM, plasma membrane; PTM, PM-tethered MYB; SIP, small basic intrinsic protein; SM, symbiosome membrane; TIP, tonoplast intrinsic protein; vasc, vascular tissue; vi-NSCC, voltage-independent nonselective cation channel; XIP, X intrinsic protein.

## Supplemental Material >

roles to AQPs, caveats must be considered, such as possible artefacts or misinterpretations and the fact that in planta functions of icAQPs are far from clear. Nonetheless, if validated, the impact on plant physiology of ion transport through AQPs could be profound. Here, we can take heed of the initial controversies surrounding cation transport via the first AQP to be identified in animals, AQP1 (1, 161, 230), contrasting with the generally accepted anion transport via AQP6 (226).

## Functional Insights from Structural Comparisons of Aquaporins

It is imperative that plant icAQPs can be reconciled with a protein structure consistent with ion transport, as has been done with animal AQPs (121, 156, 215, 232). The structural design of AQPs has been well conserved through evolution, as seen in AQP structures from bacteria, Protista, invertebrates, vertebrates, and plants. Vascular plants have accrued an expanded complement of AQPs compared to animals, for example, with 35 genes in *Arabidopsis* (90) and up to 88 in *Nicotiana tabacum* (2, 42). There are only 13 in humans (86), 3 of which can be assigned as icAQPs (AQP0, AQP1, and AQP6) (229); thus, it is not surprising that some plant AQPs can demonstrate ion transport. An expanding portfolio of available crystal structures is revealing subtle differences that can account for variations in substrate selectivity (60, 99, 120), as well as the gating processes that open and close intrasubunit water pores (55, 58, 138, 188) (**Figure 2**). Motifs are recognized that correlate with the selectivity of the intrasubunit pore (8, 81). Equivalent motifs have not been identified for ion permeation in icAQPs, though single-residue mutations in mammalian AQPs can alter ion conductance properties (121, 156). The conserved AQP monomer structure illustrated by the structures of spinach SoPIP2;1 (138, 188) (**Figure 2a,b**), *Arabidopsis* AtPIP2;4 (206) and AtTIP2;1 (99) features six hydrophobic transmembrane (TM) helices (TM1–TM6), with cytoplasmic amino (N)- and carboxyl (C)-terminal domains. Five loops (LA, LB, LC, LD, and LE) connect the TM helices, with LA, LC, and LE located extracellularly. Short helices on LB and LE fold halfway into the membrane, each carrying an NPA (asparagine-proline-alanine) signature motif (with some variations in different subfamilies) meeting in the center to create an hourglass-shaped hydrophobic intrasubunit pore (93). The NPAs in concert with four aromatic

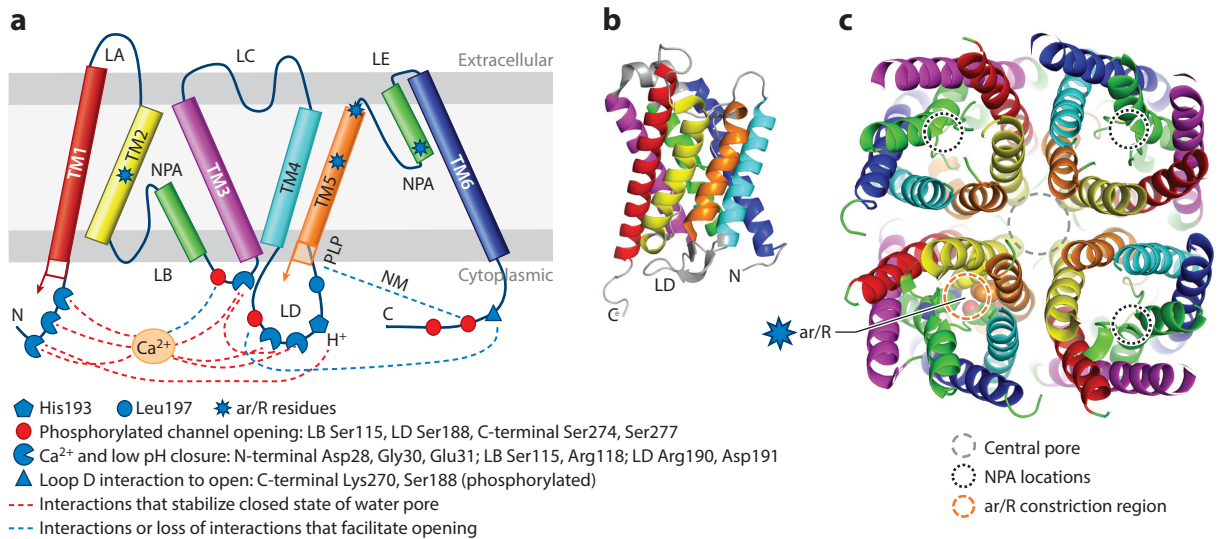


**Figure 2**

Features of PIP2 AQPs with structural information from the open and closed intrasubunit (water) pores of SoPIP2;1 (58, 138, 188). (a) Transmembrane-spanning helices (TM1–TM6), half-helices forming the hourglass structure (*green*), and NPA selectivity regions and loops (LA–LE). The intrasubunit pore (water channel) is gated via the movement of LD and stabilized in the closed state by interactions between residues on LD, LB, and the N terminus. Ca<sup>2+</sup> (Cd<sup>2+</sup> in structure 1z98) might be coordinated by these negative-charged residues on the N terminus and LD stabilizing the closed state. Protonation of His193 (LD) also stabilizes the closed state via interaction with the N terminus. The intrasubunit pore is closed by Leu197 of LD forming a hydrophobic plug. Open state is stabilized by phosphorylation of Ser115 and Ser274 (but is not observed with phosphomimetic mutants); phosphorylation of Ser188 on LD opens the intrasubunit pore (138). TM1 and TM5 move out of the membrane by half a turn when the intrasubunit pore is open. Phosphorylated Ser274 interacts with an NM near the PLP motif at the N terminus of TM5. (b) The arrangement of the monomer with TMs is indicated in the same colors as in panel a. Panel b was created using PyMOL. (c) The homotetramer of SoPIP2;1 in a cutaway view from the cytosolic side showing the location of NPAs and ar/R constriction region (60) in one monomer towards the extracellular side. Abbreviations: AQP, aquaporin; ar/R, aromatic and arginine; NM neighboring monomer; NPA, asparagine-proline-alanine; PLL, proline-leucine-proline; TM, transmembrane.

and arginine (ar/R) residues (distributed across TM2, TM5, and LE) ring the outer half of the pore and also impart substrate selectivity (63) (Figure 2c). AQPs assemble as tetramers of homomers or heteromers (14, 21, 207) and thus have four intrasubunit pores through which water diffuses in orthodox AQPs (27). A conspicuous fifth pore in the axis of tetrameric symmetry (the central pore) has been found to contain water, lipids, solvents, and ions, in various crystal structures, and is linked to ion permeation in AQP1 (231) (Figure 2c).

## The Challenge of Multiple Transport Substrates and Diverse Roles

In plants, AQPs transport neutral molecules that are required on a macroscale for growth (water, CO<sub>2</sub>, and NH<sub>3</sub> or urea) as well as micronutrients, toxic elements, waste products, signaling molecules, and ions. In addition to water, the neutral solutes transported by different AQP isoforms range over varied permeability levels: from highly lipid permeable gases (e.g., O<sub>2</sub>, CO<sub>2</sub>, and NH<sub>3</sub>) (83, 124, 197, 240) to hydrogen peroxide (H<sub>2</sub>O<sub>2</sub>) (24, 206), organic nitrogen (urea) (122), metalloids [e.g., boron as boric acid and silica as orthosilicic acid (89, 147)], protonated organic acids [e.g., lactic acid (38)], and organic metal complexes [e.g., Al malate (208)]. An impressive range of substrates can be found to permeate a single AQP; for example, AtPIP2;1 transports

**Tetramer:** oligomeric protein formed from four monomers (protomers) or subunits

**Homomer:** complex composed of more than one copy of a single type of monomer

**Heteromer:** complex composed of different subunits of monomers

---

**Central pore:** a pore within the central axis of the tetramer of an aquaporin

**PTM:** posttranslational modification

**PPI:** protein-protein interaction

---

CO<sub>2</sub> (205), possibly via the central pore (3), as well as water, H<sub>2</sub>O<sub>2</sub>, and cations (32) (**Figure 1**). This wide range in solute selectivity for one isoform may be conditional and under tight control depending on location, environmental conditions, time, and developmental context. Redundancy between AQP isoforms in terms of selectivity profiles (67) could provide a portfolio of overlapping properties enabling roles to be tailored based on the locations of the channels within the plant (**Figure 1**).

Control of the specialized properties of AQP-mediated transport can be regulated at multiple levels, including transcription (224, 239), posttranslational modification (PTM) (45, 82, 153, 170, 174), heterooligomerization (52, 222, 233), and protein-protein interactions (PPIs) that affect membrane targeting (70, 71, 109) and levels of activity (97, 115, 205). AQP sensitivity to activation or inhibition by calcium or pH (32, 140, 189, 200, 202, 221) offers dynamic layers of modulation. AQP-mediated transport of signals such as H<sub>2</sub>O<sub>2</sub> (23, 24, 48, 53, 209) and nitric oxide (207) has clear relevance for control and systemic integration of responses. The regulatory roles of the interactions of AQPs with many dissimilar proteins (15, 97, 115) or mRNA (162) remain to be explored. In association with interacting proteins, plant AQPs have been proposed as constituents of functional complexes such as a drought-sensing unit (236), CO<sub>2</sub>-sensing unit (205), or metabolon (128).

Here, consideration is given to each of the icAQPs so far identified (or indicated) with their ion conductance features integrated with previously proposed functions in the plant. This entails discussion of their structure, regulation, and similarity with ion channels in plants revealed biophysically but, so far, not identified genetically. This leads to several testable hypotheses on the function of each of the isoforms discussed in a large range of plant physiological functions ranging from signaling, osmoregulation or turgor regulation, nitrogen assimilation, and water-ion coupling.

## PLANT ION-CONDUCTING AQUAPORINS

### Tonoplast Intrinsic Proteins

A member of the tonoplast intrinsic protein (TIP) subfamily, *Arabidopsis*  $\gamma$ -TIP (AtTIP1;1), was the first recognized plant water channel AQP (131). Heterologous expression of AtTIP1;1 complementary RNA (cRNA) in *Xenopus laevis* oocytes demonstrated an osmotically induced water channel comparable to that seen for human AQP1 (155). No ion currents were observed in either isotonic or hypotonic conditions during water flow (131). After this landmark publication, it was generally accepted that ions would not permeate via plant AQPs, and reported tests for ion conductance in the literature are rare for plant AQPs (43, 77, 179). AtTIP1;1 was subsequently shown to also transport H<sub>2</sub>O<sub>2</sub> and NH<sub>3</sub> (220); it would seem that our knowledge of substrate selectivity in AQPs necessarily depends on what has been tested.

**TIP2;1 and NH<sub>4</sub><sup>+</sup> currents.** Several TIPs serve as good NH<sub>3</sub> transporters, including AtTIP2;1 (124) and the wheat homolog TaTIP2;1 (87). Both TaTIP2;1 and a rat AQP8, when expressed in *Xenopus laevis* oocytes, enabled inwardly directed ion currents when NH<sub>4</sub><sup>+</sup> was present in the external solution (77). Based on measurements of oocyte swelling simultaneously with NH<sub>4</sub><sup>+</sup>-induced inward currents and external pH, the most parsimonious interpretation indicated that both NH<sub>3</sub> and NH<sub>4</sub><sup>+</sup> were transported by TaTIP2;1. A preferred model envisioned an NH<sub>3</sub>-gated NH<sub>4</sub><sup>+</sup> conductance, in which NH<sub>3</sub> first binds to a site in the intrasubunit pore, then protons enter, associate with NH<sub>3</sub>, and move across the pore as NH<sub>4</sub><sup>+</sup>. Because NH<sub>3</sub> does not share the dipole properties of water, it was thought not to require the reorientation needed for water to pass the NPA selectivity filter, allowing NH<sub>3</sub> to retain a proton interaction throughout the pore. Both

NPA (**Figure 2a,c**) and ar/R selectivity filters are important for proton and ion exclusion in water pores (14).

A transport rate of  $\text{NH}_4^+$  in a single TIP2;1 channel was estimated at  $50 \text{ s}^{-1}$ , based on the whole-cell currents and the probable density of TIP2;1 expressed in the oocyte membrane, assuming a channel density and unitary water transport rate similar to those of AQP1 (but see 99). This estimate at  $50 \text{ s}^{-1}$  is strikingly low compared to the conductance of a moderately sized ion channel (2 pA, approximately  $10^7$  ions per second). Water flux is even faster, approximately  $10^9$  molecules per second per subunit in AQP1 (103). An alternative explanation might be that only a small fraction of the total population of water channels are available for gating as ion channels (231).

**AQP8, a TIP2;1 model in bilayers?** AQP8, like TaTIP2;1, appeared to carry  $\text{NH}_4^+$  currents when expressed in *Xenopus* oocytes (77). Purified AQP8 protein in an artificial bilayer membrane showed water and  $\text{NH}_3$  fluxes, but no single ion channel currents were observed (176), contrasting with the currents observed for AQP1 using the same technique (175). The water: $\text{NH}_3$  selectivity ratio was about 1:2 (176). Similar properties might be presumed to apply to TaTIP2;1 and AtTIP2;1. Alternative explanations have been suggested for the observed ion currents in oocytes; for example, endogenous currents might be activated by low pH near the membrane, or an inward proton current might be activated to counteract increased cytosolic pH caused by  $\text{NH}_3$  influx (14), or TaTIP2;1 might induce a parallel trafficking of endogenous oocyte channels to the membrane (176). When a mutated TaTIP2;1 was expressed in oocytes, it did not transport  $\text{NH}_3$  or show ion currents (77) but still transported water, indicating it was routed to the plasma membrane yet did not pull along an endogenous transporter. However, the possibility that  $\text{NH}_3$  entry stimulates a native channel remains to be addressed.

**TIP2;1 structure and gating.** The structure of AtTIP2;1 resolved at  $1.18 \text{ \AA}$  provided insight into features of an  $\text{NH}_3$ -transporting AQP (99). This revealed an extended ar/R selectivity filter and a wider pore as compared with PIPs and AQP1. Molecular dynamics (MD) simulation supported fluxes of water and  $\text{NH}_3$ , but not  $\text{NH}_4^+$ , via the intrasubunit pore and suggested a cytosolic gating mechanism based on sporadic pore blockade by a histidine residue, H81 (120). The importance of the extended selectivity filter was demonstrated by mutating equivalent residues in AQP1, creating an  $\text{NH}_3$ -conducting channel (99). In the solved structure, there was an interesting side channel filled with water that connected the vacuole side of the pore to the selectivity filter (99). This was speculated to be a possible pathway for  $\text{H}^+$  such that  $\text{NH}_4^+$  might enter the pore from the vacuole side and deprotonate to  $\text{NH}_3$  with the protons exiting back to the vacuole via the side pore. The vacuolar side of the pore was negatively charged and attracted  $\text{NH}_4^+$  in the MD simulations. There is similarity between this hypothetical mechanism and the model presented in Reference 77 for  $\text{NH}_3$ -gated  $\text{NH}_4^+$  permeation via TaTIP2;1.

The grapevine VvTIP2;1 is closely related to AtTIP2;1 and TaTIP2;1, with identical selectivity residues, and shows 93% sequence similarity to AtTIP2;1. Interestingly, VvTIP2;1 is gated by pH (113). Sensitivity to changes in pH would be important for  $\text{NH}_3/\text{NH}_4^+$  permeation. In yeast cells expressing VvTIP2;1, acidification of the cytoplasm decreased water permeability, while high water permeability was maintained with an acidic pH in the external medium corresponding to the vacuole (113). His131 was identified as the pH-sensitive gating residue, a position involved in the selectivity filter of AtTIP2;1 (99). Dissection of pH-dependent gating of  $\text{NH}_3$  permeation will be difficult to analyze in heterologously expressing cells or in artificial systems due to the nonindependence of permeation from changes in pH.

---

**Hypoosmotic:**

a solution diluted with water to reduce the concentration of solute below normal physiological levels

**Nonselective cation channel (NSCC):**

an ion channel that shows relatively low selectivity between cations

**Channel open probability ( $P_{\text{open}}$ ):**

the open probability of a channel measured as the proportion of time that the channel spends in its open or conducting state

---

**Posttranslational modifications may explain discrepancies.** Although the weight of evidence indicates that TIP2;1 (or AQP4) in its purified form does not transport  $\text{NH}_4^+$ , it is possible that full channel functionality depends on signaling cascades or regulatory factors. TIP2;1 in vivo might be modified or interact with an intracellular messenger, analogous to the phosphorylation-dependent activation of the ion conductance in PIP2s (158, 190) or the guanosine 3',5'-cyclic monophosphate (cGMP) activation of an ion conductance in AQP1 (6, 175). The TIP2;1 channel analyzed in the oocyte might differ from the protein purified and incorporated into bilayers or crystallized. There also remains the possibility that the central pore may allow  $\text{NH}_4^+$  permeation.

**Proposed roles for TIP2;1.** Multifunctionality appears to be a feature of AtTIP2;1 since its water permeation is implicated in the emergence of lateral roots (163) and  $\text{NH}_3$  permeation for the storage of  $\text{NH}_4^+$  in the vacuole by acid trapping (87, 124) (Figure 1k). Ammonium ( $\text{NH}_4^+$ ) release from the vacuole would not seem to be compatible with the prevailing evidence unless AtTIP2;1 can under some circumstances transport  $\text{NH}_4^+$ .

TIPs have been linked to ion transport during stomatal closure (Figure 1b). VvTIP2;1 is highly expressed in grapevine leaves and shows a strong positive linear correlation to stomatal conductance during water stress and recovery (150). Efflux of  $^{86}\text{Rb}^+$  as a tracer for  $\text{K}^+$  from the vacuole of *Commelina communis* guard cells revealed sensitivity to hypoosmotic gradients that induced water flow into the vacuole (125). A TIP was implicated as either a sensor or both a sensor and an actuator of a water flow-sensitive ion channel (125). It was later shown that the hypoosmotic-sensitive efflux was inhibited by acidic cytoplasmic pH (126). Both tonoplast water permeability (5) and VvTIP2;1 water permeability (113) are inhibited by cytosolic acidification. VvTIP2;1, when expressed in yeast and subject to hypotonic shocks, facilitated higher water permeability with increased membrane tension or tonicity (112). AQPs could be osmosensors or turgor sensors (76) and a possible example of this is the rose RhPIP2;1 as a component of a drought sensor system (236) (Figure 1c). It would seem that TIP2;1 is a strong candidate for the sensor on the tonoplast suggested by MacRobbie (125), and further research is required to investigate its potential to regulate or mediate  $\text{K}^+$  and/or  $\text{NH}_4^+$  efflux from the vacuole.

**Unidentified nonselective cation channel in the tonoplast: the fast vacuolar channel.** A prominent nonselective cation channel (NSCC) in the tonoplast of plant cells is the fast vacuolar (FV) channel, characterized by fast activation for both positive and negative voltage steps as opposed to the voltage-dependent slow-activating (SV) channel (75). The FV channel has not been molecularly identified, while the SV channel is attributed to the *TWO-PORE CHANNEL 1 (TPC1)* gene in *Arabidopsis* (144). There are features of the FV channel that are similar to the pattern emerging for NSCCs attributed to some PIPs and AQP1: inhibition by  $\text{Ca}^{2+}$  ( $K_d = 6 \mu\text{M}$  for barley FV) (187) and inhibition by  $\text{Mg}^{2+}$  at higher concentrations (29). The selectivity of the FV channel to monovalent cations  $\text{NH}_4^+ > \text{K}^+ \geq \text{Rb}^+ \geq \text{Cs}^+ > \text{Na}^+ > \text{Li}^+$  (30) is also relevant regarding the possible  $\text{NH}_4^+$  permeation through TIP2;1. The FV channel has a unique sensitivity of the channel open probability ( $P_{\text{open}}$ ) to  $\text{K}^+$  concentration, proposed to regulate the release of  $\text{K}^+$  from the vacuole (149). Relevant here is the barley HvPIP2;8, which displays a complex interaction between  $\text{K}^+$  and  $\text{Na}^+$  (190), setting a precedent for possible  $\text{K}^+$  regulation in other icAQPs. Biophysical features of FV channels warrant comparison to any ion-conducting TIPs that may be characterized in the future.

**NOD26: A NIP for  $\text{N}_2$ -Fixing Symbiosis**

The NIP subfamily is relatively large, and many have been shown to be expressed on the plasma membrane and responsible for neutral metalloid transport (57, 148). Nodulin 26, the archetype of

the NIP family of AQPs, is located on the symbiosome membrane (SM) in nitrogen-fixing legume nodules (54) and when purified and incorporated into lipid bilayers, nonselective (slightly more anion than cation) ion channels were observed (110, 210). There is one report of unpublished data stating that no ion currents were observed when NOD26 was expressed in *Xenopus* oocytes, though the conditions were not reported (e.g., divalent concentration, pH, etc.) (43). NOD26 displays modest water channel activity (165) and is permeable to glycerol (43), formamide, and acetamide but not urea (165). Ammonia permeability of the SM is mediated by a mercury-inhibited channel (136), and NOD26 incorporated into lipid vesicles induces a fivefold higher  $\text{NH}_3$  permeability than that for water (83). Transporters on the SM carry out the exchange of fixed carbon as malate for reduced  $\text{N}_2$  as  $\text{NH}_3/\text{NH}_4^+$  from the bacteroids (39). Glutamine synthetase is the first enzymic reaction in the ammonia assimilation pathway, and it binds to the C terminus of NOD26 located in the cytosol. Given the  $\text{NH}_3$  permeability of NOD26, researchers therefore proposed that NOD26 plus bound glutamine synthetase functions as a metabolic funnel to efficiently transport and assimilate  $\text{NH}_3$  and to reduce  $\text{NH}_3$  toxicity in the cytoplasm (128) (**Figure 1j**).

**Unidentified molecular transporters on the symbiosome membrane.** Several transport systems have been identified on the SM that supply the bacteroids with the required nutrients for  $\text{N}_2$  fixation, but the molecular identity of the key transporters for malate and  $\text{NH}_4^+$  are still outstanding (39). The SM is energized by an  $\text{H}^+$ -ATPase such that the space between the bacteroids and the SM (symbiosome space) is acidic and the membrane potential is negative (39). An NSCC with a preference for  $\text{NH}_4^+$  ( $\text{NH}_4^+$ -NSCC) (selectivity:  $\text{NH}_4^+ > \text{K}^+ = \text{Na}^+ > \text{Rb}^+ > \text{Cs}^+ > \text{methylamine}^+$ ) (139, 166) was identified on the SM of both soybean and *Lotus japonicus* nodules using patch clamp (166, 193). This channel was blocked by  $\text{Ca}^{2+}$  and  $\text{Mg}^{2+}$  (139, 166, 193). Under in vivo conditions  $\text{Mg}^{2+}$  would normally gate the channel to allow one-way  $\text{NH}_4^+$  permeation to the cytoplasm (166). This channel has a high density on the membrane and exhibits cooperative gating (139). It has a very small single-channel conductance that could only be resolved by noise analysis (139, 193).

**Could NOD26 be the  $\text{NH}_4^+$ -NSCC on the symbiosome membrane?** NOD26 channels in lipid bilayers, although of large conductance (3.3 nS in 1 M KCl) (210), showed numerous smaller substates (<20 pA in some records) and voltage dependency when phosphorylated at a C-terminal site, which is normally regulated by a  $\text{Ca}^{2+}$ -dependent protein kinase (110). Phosphorylation of NOD26 was also shown to enhance its water permeability when expressed in *Xenopus* oocytes (68). The slight anion selectivity over cations for NOD26 channels (210) contrasts with the  $\text{NH}_4^+$ -NSCC that has higher cation-to- $\text{Cl}^-$  selectivity (193), but the substate fluctuations are similar to those observed for the  $\text{NH}_4^+$ -NSCC (139). It was previously hypothesized that NOD26 may be the SM malate transporter based on the slightly higher anion selectivity of NOD26 in bilayers and its phosphorylation response (141, 210). However, it is unclear what type of ion channel phenotype will be observed for glutamine synthetase (GS)-bound NOD26 in more physiological solutions and with divalents present, since the buffers used for the bilayer experiments had only 8  $\mu\text{M}$  of free  $\text{Ca}^{2+}$  on both sides of the membrane with 1 M KCl (210). The large osmotic pressure with 1 M KCl is likely to have had a profound effect on NOD26 as a water channel (199, figure 2b; 227) that may also impact its ion-channel phenotype.

Given the unfavorable gradients for  $\text{NH}_3$  out of the symbiosome space but favorable gradients for  $\text{NH}_4^+$ , it would seem more efficient if NOD26 were permeable to  $\text{NH}_4^+$ . It was suggested that the  $\text{NH}_4^+$ -NSCC in concert with the  $\text{NH}_3$  permeation via NOD26 and the proton pump could otherwise result in a futile cycle across the SM (128). The GS and NOD26 metabolon makes NOD26 a candidate for the  $\text{NH}_4^+$ -NSCC, especially since the substrate for GS is  $\text{NH}_4^+$  (50).

---

#### Single-channel conductance:

electrical conductance of a single ion channel normally measured in units of picosiemens (pS; Siemens = amps per volt)

---

**Single-channel events:** step-like fluctuations in membrane current corresponding to the opening and closing of single ion channels normally measured as picoamperes (pA)

Although there are other AQPs on the SM, including a TIP2 and PIP2 (214), NOD26 is a prime candidate for the  $\text{NH}_4^+$ -NSSC.

### VvXIP1 Facilitates Copper and Nickel Transport

VvXIP1 expressed in yeast enabled transport of copper, arsenic, and nickel, and it was suggested that VvXIP1 may be able to transport  $\text{Cu}^{2+}$  and  $\text{Ni}^{2+}$  ions (137). The XIPs consisting of between 1 and 8 members occur in eudicot species (20, 40, 42). They are characterized by the NPARC motif in LE, a more variable NPA motif in LB, and a longer LC (20, 42). There is wide diversity among this subfamily, with expression in the plasma membrane (NtXIP1, StXIP1) (21), endoplasmic reticulum, and perhaps the tonoplast (VvXIP1) (137) and for NtXIP1 in specific cell types throughout the plant, including root tip and guard cells (21). They have permeability to more bulky neutral solutes but no detectable water permeability (21, 137). Based on the ar/R residues, selectivity has been predicted for boric acid, urea, and  $\text{H}_2\text{O}_2$  (2). Expression of VvXIP1 in cultured cells of grape was downregulated in the presence of copper (100  $\mu\text{M}$ ) and NaCl (100 mM) and strongly by abscisic acid, while in vine leaves it had reduced expression under water stress, suggesting a role in osmoregulation (137). Copper and nickel ions form uncharged complexes with organic compounds (73), and these could be taken up as uncharged complexes as occurs with Al-malate complexes through AtNIP1;2 (208). Until specific electrogenic transport is demonstrated for VvXIP1, it is not certain that it may permeate uncomplexed ions.

### OsPIP1;3: A Multifunctional Water and Anion Channel?

A rice PIP1 (OsPIP1;3*in*) from a drought-resistant rice (*indica*) cultivar elicits anion currents when expressed in mammalian HEK293 cells (123). The *OsPIP1;3in* gene had single-nucleotide polymorphisms resulting in some differences in the protein as compared to the OsPIP1;3*jp* (*japonica*) previously characterized (129). The OsPIP1;3*jp* protein expressed in *Xenopus* oocytes did not elicit significant water permeability but did interact with some OsPIP2 members (OsPIP2;2 and OsPIP2;4 but not OsPIP2;3) to increase water permeability (129), in line with similar observations for PIP1 members more generally (25; but see 235). In the later work (123), OsPIP1;3*in* function in *Xenopus* oocytes was confirmed, but it was also shown to function as a water channel in its own right when purified and incorporated into proteoliposomes. The anion currents were observed with an N-terminal-tagged green fluorescent protein (GFP) OsPIP1;3*in* expressed in HEK293 cells using whole-cell patch clamp (123). The whole-cell currents displayed high selectivity for  $\text{NO}_3^-$  relative to  $\text{HCO}_3^-/\text{CO}_3^{2-}$ .

**Does PIP1;3 act alone in planta?** It is clear that PIP1 members transit to the plasma membrane more consistently when in association with certain PIP2 members (18, 25, 52, 233). The coexpression of PIP1 and PIP2 has been shown to affect the selectivity for ions (32) and  $\text{CO}_2$  (140). This is pertinent for the discussion of OsPIP1;3, since it may only exist in the plasma membrane as a heterotetramer with a PIP2. However, the rice PIP1s can go to the *Xenopus* oocyte plasma membrane without a PIP2 helper (235). An expression network of OsPIPs in rice roots from various cultivars revealed a significant correlation between expression of OsPIP1;3 and OsPIP2;2 under well-watered conditions (65); OsPIP2;2 is one of the partners that enhances water transport in *Xenopus* oocytes when coexpressed (129). It remains to be seen if the anion conductance observed for OsPIP1;3*in* still occurs when interacting with OsPIP2s. Heterotetramers formed between a cation conducting PIP2 and an anion conducting PIP1 may show interesting ion transport features.

**The AQP6 parallel.** Anion conductances and single-channel events have been shown for mammalian AQP6 expressed in different heterologous cells (225). AQP6 colocalizes with an  $\text{H}^+$ -ATPase

to intracellular compartments in acid-secreting kidney cells (225) but expresses in the plasma membrane of *Xenopus* oocytes (226). Interestingly, AQP6, like OsPIP1;3*in*, required a GFP on the N terminus to go to the plasma membrane of HEK293 cells (13, 84). Both AQP6 water permeability and voltage-independent anion currents are activated in the presence of Hg<sup>2+</sup> or low pH and maximally activated at pH 4 (226). The P<sub>Na+</sub>:P<sub>Cl-</sub> ratio of AQP6 in oocytes was 0.28, but mutation of a unique positively charged residue (Lys72) that occurs in the cytoplasmic vestibule of the water pore to a negative charge (Lys72Glu) resulted in greater Na<sup>+</sup> permeability (P<sub>Na+</sub>:P<sub>Cl-</sub> = 1.13) (226). When examined with patch clamp, wild-type AQP6 activated by Hg<sup>2+</sup> showed equal permeability for Na<sup>+</sup> and Cl<sup>-</sup>. The intrasubunit pore was assigned as the pathway for ions based on the dose-response curve for Hg<sup>2+</sup> activation (74).

The contact point between TM helices 2 and 5 was shown to be important for anion conductance through AQP6 (121). By changing Asn60 to a Gly corresponding to the highly conserved residues in most mammalian AQPs, anion transport was abolished and high water permeability was established (121). The reverse was demonstrated for AQP5, where AQP5 was turned from a water channel to an anion channel by mutating Leu51 corresponding to residue 61 in AQP6 (156), one residue from Asn60. The Leu51 (L51) side chains project into the central pore, and it was suggested that the mutation to Arg (R), imposing four positive charges into the central pore, would distort the AQP to reduce water conductance and to increase anion conductance (156). AQP5 shows CO<sub>2</sub> and NH<sub>3</sub> permeability, but the L51R mutation interfered with CO<sub>2</sub> transport. It was concluded that part of the anion conductance occurred via the intrasubunit pore, based on inhibitor effects, but some could be attributed to the central pore given that the L51R made the central pore more hydrophilic. This also explained the reduced CO<sub>2</sub> permeability if CO<sub>2</sub> permeated the central pore. Interestingly, when the same oocytes were measured for water permeation and ion conductance with the different mutations at Asn60, an inverse water:anion permeability relationship was observed where water permeability declined with increasing anion conductance, similar to what has been observed for AtPIP2;1 and HvPIP2;8 with mutations in C-terminal serines (158, 190) (**Figure 3a**).

Given the wealth of information available for the mammalian AQP6 and mutated AQP5 anion conductance, it is instructive to examine the corresponding residues for OsPIP1;3*in*. The corresponding residues in OsPIP1;3 reveal the conserved water channel type rather than the AQP6 type, but four consecutive positively charged Arg residues occur in the N terminus of OsPIP1;3*in* that are not present in OsPIP1;3*jp* as well as a Ser to Arg substitution in LA. A comparison of the anion conductance of OsPIP1;3*in* with that of OsPIP1;3*jp* could shed some light on the structural requirements for anion conductance.

**Proposed roles of OsPIP1;3.** OsPIP1;3 has the hallmarks of a multifunctional AQP. It is one of 34 genes encoding AQPs in rice: 12 are classified as PIPs, with 3 designated as PIP1 (PIP1;1, PIP1;2, PIP1;3) and 9 as PIP2 (69, 135, 172). OsPIP1;3 is localized mainly at the proximal end of the endodermis of the root and the cell surface around the xylem (123). Its expression differs between lowland (*japonica*) rice and upland (*indica*) rice that shows drought avoidance characteristics (118, 119). The *japonica* OsPIP1;3*jp* expression levels were correlated with differences in survival at cold temperatures between cultivars, and overexpression in rice enhanced chilling tolerance (129). In response to salinity, OsPIP1;3*jp* was the only PIP to show continuous downregulation over 24 h (69). In apparent contradiction to the effects of salinity, root OsPIP1;3 is upregulated by osmotic stress in *indica* (20% polyethylene glycol) but does not change in *japonica*, a feature also of OsPIP1;2, OsPIP2;1, and OsPIP2;5 (118). When OsPIP1;3 was expressed under the control of a stress-inducible promoter in *japonica*, it conferred drought avoidance characteristics, including higher osmotic root hydraulic conductivity after osmotic stress compared to wild-type *japonica*

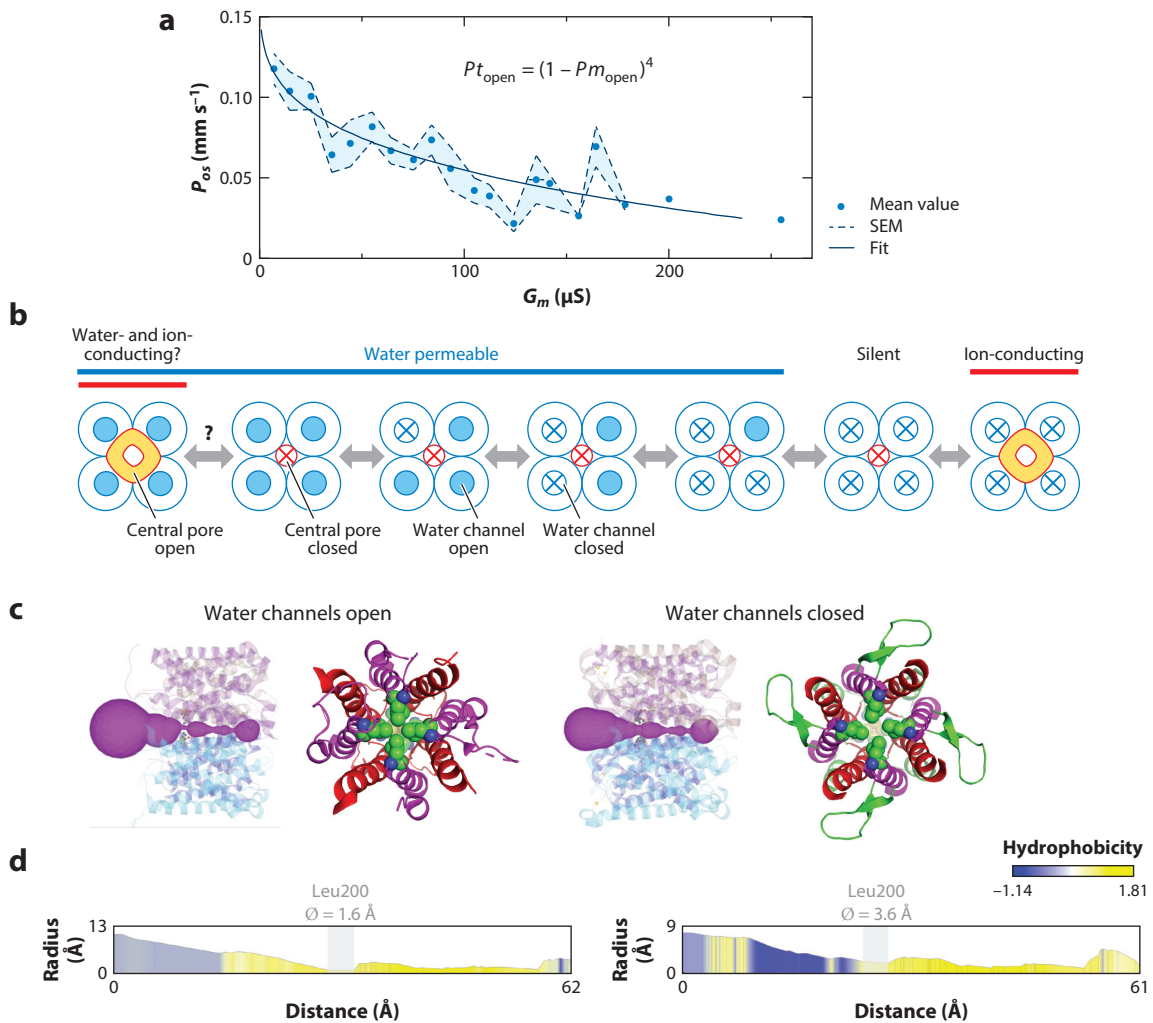


**Figure 3**

Model of ion channel gating through PIP2;1. (a) Inverse relationship between water permeability ( $P_{os}$ ) and membrane ion conductance ( $G_m$ ) for *Xenopus* oocytes expressing AtPIP2;1 wild type and mutants (S280D, S283D, and S280DS283D). Data from Reference 158. The gating model for open probability of the tetrameric central pore (ion conducting,  $P_{t_{\text{open}}}$ ) is fitted to the data. See also **Supplemental Information**. (b) Possible transitions in gating between water-conducting monomers to the ion-conducting central pore. An intermediate silent mode might account for the low ion channel open probability, and the open ion channel might show multiple substates (175). (c) The central pore on the open and closed channel structures of SoPIP2;1 [open 2b5f, closed 1Z98 (188)]. Structures analyzed with MOLEonline (154). Similar results were obtained with PoreWalker (145). The purple connected spheres indicate the diameters along the central pore. Leu200 on each monomer constricts the pore at the cytoplasmic end of TM5. The movement of loop D from the open water channel state to the closed state results in a change in the constriction at Leu200 that widens the central pore, matching the inverse gating model in panel a. Only TM2, TM5 (lining the central pore), and loop D are shown, looking down the central pore from the cytoplasmic side with the Leu200 side chain shown as spheres. Panel adapted from images created with PyMOL. (d) Variation in radii of the central pore along the length of the channel for open and closed states of SoPIP2;1 (2b5f & 1Z98). Data obtained from the output of MOLEonline. The diameter at the Leu200 constriction is indicated. Shading indicates the hydrophobicity of the residues lining the pore. Abbreviations:  $G_m$ , oocyte electrical conductance (units microSiemens);  $P_{os}$ , osmotic water permeability;  $P_{t_{\text{open}}}$ , open probability of the central tetrameric pore for ion flow;  $P_{m_{\text{open}}}$ , open probability of the monomeric (intrasubunit) water conducting pore;  $\varnothing$ , diameter; SEM, standard error of the mean.

**Supplemental Material** >

(119). When ectopically expressed in tobacco, OsPIP1;3*in* increased root hydraulic conductivity, photosynthesis, and water use efficiency (123). Based on the apparent increase in leaf mesophyll conductance to CO<sub>2</sub> in the transgenics (but see 104), OsPIP1;3 expression in a cyanobacterium was also found to affect growth, indicative of a role in CO<sub>2</sub> transport (123).

OsPIP1;3 has been linked to the virulence of *Xanthomonas oryzae* that causes bacterial blight in rice (116). One-domain hairpin proteins, such as Hpa1 from gram-negative bacterial pathogens, are required to form the translocators in the plant plasma membrane for the injection of bacterial effector proteins. Hpa1 interacts with AtPIP1;4 and OsPIP1;3 to allow the import of a bacterial effector PthXo1, a transcription activator (115, 116). This is dependent on the specific interaction between Hpa1 and LE of OsPIP1;3 (116). It is not known how OsPIP1;3-Hpa1 interaction mediates effector translocation, but it would be interesting to determine if the anion channel function of OsPIP1;3 is involved or altered in the association.

**Unexplained anion channels and the water:NO<sub>3</sub><sup>-</sup> link.** Anion channels have been observed in protoplasts derived from plant roots using patch clamp, and among these are several that show high NO<sub>3</sub><sup>-</sup> permeability (9). One type observed in several species is the outward-rectifying depolarization-activated anion channels (OR-DAACs) (185). These show similarity to the anion currents shown for OsPIP1;3*in* (123, 182). OR-DAACs are a potential pathway for anion uptake into roots cells under luxuriant external NO<sub>3</sub><sup>-</sup> or under salinity stress as a passive pathway for Cl<sup>-</sup> entry (182). There is a strong link between NO<sub>3</sub><sup>-</sup> supply to roots and water transport via root AQPs (194; see, e.g., 62, 114). OsPIP1;3*in* and related homologs in other plants could have undiscovered roles in water and NO<sub>3</sub><sup>-</sup> uptake in roots.

### The Cation-Conducting AtPIP2;1, AtPIP2;2, and HvPIP2;8

Two closely related members of the PIP2 group from *Arabidopsis*, AtPIP2;1 and AtPIP2;2, as well as barley HvPIP2;8 display nonselective voltage-independent cation conductances when expressed in *Xenopus laevis* oocytes (32, 101, 158, 190). The AtPIP2;1 cation conductance is inhibited by external divalent cations (101) and low pH (32) similar to the inhibition of water permeability seen with the same purified protein in proteoliposomes (200). The cation conductance of AtPIP2;2 proved to have a lower inhibitory constant for external Ca<sup>2+</sup> compared to that of AtPIP2;1 (101). In contrast, AtPIP2;7 conferred high water permeability when expressed in *Xenopus* oocytes but did not show cation conductance under the same conditions (101). An interesting feature of PIP2;1 and PIP2;2 is the voltage-dependent block by some divalents (101). External barium blocks the inward current and results in a time-dependent outward current. There is also a competitive interaction between Ca<sup>2+</sup> and Ba<sup>2+</sup>, suggesting that they act at the same site (101).

The barley HvPIP2;8 was identified from a survey of most of the barley PIP1 and PIP2 members expressed in *Xenopus* oocytes as the only icAQP (190). It was also inhibited by external divalents (Ba<sup>2+</sup>, Ca<sup>2+</sup>, and Cd<sup>2+</sup>), and, similar to AtPIP2;1, there was an interaction in this case between Mg<sup>2+</sup> and Ca<sup>2+</sup>. There was also an interaction between Na<sup>+</sup> and K<sup>+</sup> for HvPIP2;8 where a mix of the two ions at a ratio of 1:1 significantly inhibited the current. Other univalent cations (Rb<sup>+</sup>, Cs<sup>+</sup>, Li<sup>+</sup>) did not elicit currents. This feature contrasts with that of AtPIP2;1, which shows significant currents with Rb<sup>+</sup>, Cs<sup>+</sup>, and Li<sup>+</sup> (J. Qiu, unpublished data) and also has opposite relative selectivity between Na<sup>+</sup> and K<sup>+</sup> (158).

**Are the cation conductances induced by AtPIP2;1, AtPIP2;2, and HvPIP2;8 artefacts?** It is unlikely that the currents observed for AtPIP2;1, AtPIP2;2, and HvPIP2;8 expressed in *Xenopus* oocytes are artefacts caused by activation of a native ion channel for the following reasons:

---

#### Outward current:

a current that is equivalent to positively charged ions leaving the cell (or negatively charged ions entering the cell) with positive sign convention

---

---

**Current-voltage**

**curve:** plot of current versus voltage obtained from a voltage clamp experiment where membrane voltage is set by injections of current

---

1. AtPIP2;2 and AtPIP2;1 show different sensitivity to block by external  $\text{Ca}^{2+}$ .
2. HvPIP2;8 shows a different ion selectivity than that of AtPIP2;1.
3. The AQP1-associated cation channel shows a selectivity for monovalent cations similar to that of AtPIP2;1 when expressed in *Xenopus* oocytes but differs in its dependence on activation by cytoplasmic cGMP (6, 175), which interacts with Arg residues on loop D (100). These residues are not present in loop D of AtPIP2;1. In contrast, AtPIP2;1 cation conductance is inhibited by cGMP (158). For AtPIP2;1, the phosphorylation of C-terminal residues and another set of unidentified sites or factors are involved in the activation of the cation conductance (158).
4. The arylsulfonamide AqB011 selectively blocks the ion conductance and not the water conductance through AQP1 (100) but has no effect on AtPIP2;1 or AtPIP2;2 (101).
5. A nonfunctional mutant of AtPIP2;1 (G103W), which localizes to the plasma membrane based on both its positive interaction with AtPIP1;2 (32) and the fluorescence signal from G103W-PIP2;1-YFP fusion proteins (205), does not elicit a cation conductance or water transport (32). Interestingly, this mutant also does not transport  $\text{CO}_2$  in *Xenopus* oocytes (205).
6. AtPIP2;1 expressed in yeast causes an increase in cytoplasmic  $\text{Na}^+$  content and a reduction in  $\text{K}^+$  content, as it does in *Xenopus* oocytes (32). It was further demonstrated that the  $\text{Na}^+$  content of a yeast mutant deficient in  $\text{Na}^+$  transport was affected by the phosphomimic mutants of AtPIP2;1 (158).

None of the above observations are consistent with AtPIP2;1/AtPIP2;2, HvPIP2;8, or AQP1 activating one particular type of endogenous channel in *Xenopus* oocytes. Oocytes do have endogenous NSCCs that can be activated by the expression of heterologous membrane proteins (183), including plant transporters (177), but most of these are reported to be activated by voltage (183), e.g., a hyperpolarization time-dependent current (195) and a low-pH-activated current carried by divalents (105). A connexin is activated at low external divalent concentrations in immature *Xenopus* oocytes and produces nonselective cation conductances (49, 238). These are inactivated at both positive and negative membrane potentials, giving a characteristic S-shaped steady-state current-voltage curve (238) that is very different to those observed for PIP2;1 (101, 158). This channel is also activated by external  $\text{H}_2\text{O}_2$  (98), and given that PIP2;1 transports  $\text{H}_2\text{O}_2$ , the expression of PIP2;1 could indirectly activate the connexin at low divalent concentrations. However, there is no effect of  $\text{H}_2\text{O}_2$  on AtPIP2;1-induced ion currents, nor any effect of externally supplied catalase (S. Tyerman and J. Qiu, unpublished data) that has been reported to strongly inhibit the connexin hemichannel in *Xenopus* oocytes (17). Also, AtPIP2;7 does not elicit ion currents (101), and this AQP has been shown to transport  $\text{H}_2\text{O}_2$  (79). The ultimate proof of ion conduction via AtPIP2;1/AtPIP2;2 and HvPIP2;8 will require the incorporation of purified protein into lipid vesicles or planar lipid bilayers to assess single-channel currents.

**Regulation of PIP2 aquaporins.** PIP2 regulation includes transcript regulation (37, 239), PTMs (45, 153, 170, 174), PPIs (15, 35, 152, 169, 186), and selective endocytosis from the plasma membrane stimulated by reactive oxygen species (127, 219). The PTMs and PPIs can affect membrane targeting, substrate selectivity, and  $\text{pH}_o$  sensitivity (71, 109, 140, 158, 198, 202, 222). PPIs between PIP1 and PIP2 members have been shown to allow movement of PIP1 members to the membrane (25, 233).

Delivery to the plasma membrane involves vesicle fusions facilitated by several proteins, including the syntaxin SNARE proteins. Two SNARE proteins (SYP61 and SYP121) physically interact with AtPIP2;7, and SYP121 interacts with maize ZmPIP2;5 (19, 70). *Arabidopsis* SYP121

also interacts with the voltage sensor domains of K<sup>+</sup> channels for membrane trafficking and modifies the voltage sensitivity and gating of the channels (64, 111). These SNARE proteins thus have the capacity to colocalize and coordinate K<sup>+</sup> and water transport for osmotic regulation. It is not known if this interaction may also impact the gating of the ion conductance via AtPIP2;1 or AtPIP2;2 should they interact with SNAREs. It is also noteworthy that *Chlorella* virus MT325 encodes both a water and a potassium channel that when expressed in *Xenopus* oocytes act synergistically, including an induced sensitivity to Ba<sup>2+</sup> for water transport (61).

**Phosphorylation is a key regulatory component of PIP2s.** As one of several kinds of PTMs, phosphorylation of PIP2 isoforms affects water transport (66, 91, 157, 198). There is considerable complexity in the regulation of PIP2s via phosphorylation since various protein kinases (PKs) have now been identified as interacting with PIP2s and phosphorylating specific or as-yet-unknown residues. Two PKs in spinach leaves phosphorylate SoPIP2;1 at either Ser115 (Mg<sup>2+</sup>-dependent) of loop B or Ser274 (Ca<sup>2+</sup>-dependent) in the C terminus to enhance water transport (181) though purified protein with phosphorylation mimics at these sites did not show enhanced water transport (138). The loop B site is conserved across all PIPs and TIPs, while the C-terminal site is conserved across PIPs and NIPs, including GmNOD26 (181). A membrane receptor kinase, SIRK1, identified as a sucrose-dependent PK interacts with five PIP2s (AtPIP2;1–AtPIP2;4 and AtPIP2;7) upon stimulation by sucrose after carbon starvation (218). SIRK1 was able to doubly phosphorylate a peptide at the equivalent S280 and S283 sites of AtPIP2;4 (218).

A PK involved in stomatal closure in response to abscisic acid, SnRK2.6 (OST1) phosphorylates AtPIP2;1 at S121 in loop B. This enhances AtPIP2;1-mediated water transport in *Xenopus* oocytes and in guard cells, as indicated from phenotypes and complementation with phosphorylation-deficient mutants and phosphorylation mimics at S121 (66). This site also appears to regulate H<sub>2</sub>O<sub>2</sub> permeation (167). Protein identification after immunopurification identified 37 putative kinases that could interact with AtPIP2;1 (15). Two members of the receptor-like kinases from *Arabidopsis*, RLK1 and Feronia, interact with AtPIP2;1 but modulate water transport in opposite directions (15). The stimulation of water transport assayed in *Xenopus* oocytes induced by RLK1 did not occur via the C-terminal S280 or S283 nor the loop B S121. Feronia inhibition of water transport depended on the C-terminal Ser280 and Ser283, and the phosphomimetic mutants (S280D-S283D) also inhibited water transport. The inhibitory effect on water transport of phosphomimetic mutations of S280 and S283 was confirmed recently, correlating with an increase in cation conductance (158).

Two *Arabidopsis* 14-3-3 proteins, GRF4 (14-3-3φ) and GRF10 (14-3-3ε), increase water transport via AtPIP2;1 in an apparently precise stoichiometry (though seemingly inhibited at higher expression levels of these 14-3-3s), preferentially when AtPIP2;1 is double-phosphorylated at S280 and S283 (152). Binding of these proteins occurs even when AtPIP2;1 is unphosphorylated at the C terminus, but it is unclear exactly where binding occurs. It appears that both phosphorylation and binding are required for the increased water transport that is suggested to occur via the gating of AtPIP2;1 (152). The interaction with these 14-3-3s is required for the diurnal rhythmicity of *Arabidopsis* rosette hydraulic conductance (152).

Apart from direct phosphorylation effects, there is a suggestion that the phospholipid signal molecule, phosphatidic acid, may also interact with AtPIP2;1 and AtPIP2;2 (133). A phospholipase D interacted with AtPIP2;1, which was decreased by treatment with H<sub>2</sub>O<sub>2</sub> (15). It is not known if phosphatidic acid modulates AtPIP2;1 transport. It would appear that there are several regulatory pathways that act via or in concert with phosphorylation on AtPIP2;1 by a range of PKs and/or by direct protein interaction. Given the different substrates that AtPIP2;1 can

transport, it would be worthwhile to determine how these phosphorylations and interactions potentially switch substrate specificity.

**Phosphorylation mimics of AtPIP2;1 and HvPIP2;8 regulate an apparent mutually exclusive ion and water conductance.** In view of the link between salinity stress, phosphorylation, and membrane-targeting of AtPIP2;1 through phosphorylation at S280 and S283 (45, 153, 196), the ion transport characteristics of AtPIP2;1 phosphorylation-mimic mutants at these sites were examined (158). The double phosphorylation-mimic mutations to aspartate (S280D and S283D, dSD) or phosphorylation-null mutations (S280A and S283A dSA) of AtPIP2;1 caused a dramatic shift in both water and ion permeation with a potentially tenfold inverse change in ion conductance and water permeability (**Figure 3a**). Depending on the combination, either a high water permeability or a high ion conductance was evident. The high ion conductance was more often associated with the dSD while the high water permeability was more often associated with dSA, though in both cases any given oocyte could show variation along an inverse trajectory of increasing ion conductance and decreasing water conductance (158) (**Figure 3a**). For the barley HvPIP2;8 a similar inverse relationship was observed for the S285D phosphomimic mutant, which was modified by the kinase inhibitor H7 indicating that other sites are involved in regulating the water:cation selectivity (190).

**The elusive voltage-independent nonselective cation channel.** The features of the univalent cation transport through AtPIP2;1 and AtPIP2;2 are similar to the voltage-independent nonselective cation channels (vi-NSCCs) observed in patch clamp measurements on root protoplasts (44, 192) that match properties observed for nonselective cation transport in roots (51). HvPIP2;8, however, has an interesting selectivity sequence that does not match known vi-NSCCs and bears a greater resemblance to the Na<sup>+</sup> and K<sup>+</sup> permeability of some high-affinity K<sup>+</sup> transporters (HKTs) (190). It has been hypothesized that AtPIP2;1 and, by association, AtPIP2;2 could account for the elusive vi-NSCC in *Arabidopsis* (32, 132). Besides the similarity in calcium- and pH-dependency between vi-NSCCs and AtPIP2;1/AtPIP2;2, they are also inhibited by cGMP (85, 158). An estimate can be made of the possible role of AtPIP2;1 as the vi-NSCC in *Arabidopsis* root protoplasts based on the scaling between water permeability and ion conductance observed in *Xenopus* oocytes with different amounts of injected AtPIP2;1 cRNA (44, 132). Even if only half of the membrane water permeability was due to AtPIP2;1, the ion conductance can account for the measured vi-NSCC conductances using patch clamp. That PIP2;1 shows a higher conductance for K<sup>+</sup> than for Na<sup>+</sup> may also be relevant to the remaining K<sup>+</sup> uptake pathway in roots that is evident when HAK and AKT K<sup>+</sup> transporters are knocked out (168). This pathway is inhibited by Ca<sup>2+</sup>, Mg<sup>2+</sup>, Ba<sup>2+</sup>, and La<sup>3+</sup> and transports Cs<sup>+</sup>, and its activity is reduced by cyclic nucleotides. There are many other known features of vi-NSCCs that remain to be tested on the icPIP2s. This includes the full selectivity sequence to different univalent cations for AtPIP2;1/AtPIP2;2 and pharmacology (44). A link with salinity stress was indicated for HvPIP2;8 where its transcript abundance increased in shoot tissue following salt treatment only in a salt-tolerant cultivar but not in a salt-sensitive cultivar (190). A receptor-like cytoplasmic kinase from rice (OsRLCK311) interacts with AtPIP2;1 and OsPIP2;1 and induces salinity tolerance in *Arabidopsis*, proposed to be via altered stomatal regulation (169). This did not seem to be related to kinase activity, since an inactive form of OsRLCK311 had the same effect. The many and varied effects of overexpression of PIPs on salinity tolerance (132) could be related to ion transport, water transport, or both in different tissues and organs, so cell-targeted and specific mutations (e.g., of particular phosphoserines) will be required to clearly demonstrate the roles in ion transport.

## Can PIP2 Structure Be Reconciled with Ion Transport? The AQP1 Parallel

AQP1 is able to facilitate nonselective univalent cation transport (230) that initially was controversial (161). It was later confirmed by independent observations (175, 237), though qualified (175) and dependent on where it is expressed (26, 191). AQP1 is now linked to biological function in fluid secretion and cancer metastasis (41, 143). The AQP1 ion conductance is activated by cGMP binding to loop D (100), primed by the phosphorylation of a C-terminal tyrosine (253), and also activated by protein kinase C (237). Single-channel events for AQP1 have been recorded in plasma membranes of *Xenopus* oocyte and choroid plexus cells having a single-channel conductance of 150 pS and 166 pS with 100 mM K<sup>+</sup> and Cs<sup>+</sup> salines, respectively (6, 26). In lipid bilayers, the single-channel conductance was lower (substates up to 10 pS in 100 mM K<sup>+</sup> or Na<sup>+</sup>) (175), perhaps due to the particular lipid composition used and mechanosensitivity (12, 142). AQP1 has a selectivity sequence of K<sup>+</sup> = Cs<sup>+</sup> > Na<sup>+</sup> > TEA<sup>+</sup> (230). While the univalent selectivity sequence of AtPIP2;1 has not yet been reported, slightly higher K<sup>+</sup> to Na<sup>+</sup> conductance has been observed (158); Rb<sup>+</sup>, Li<sup>+</sup>, and Cs<sup>+</sup> also permeate (J. Qiu, unpublished observations) and show some similarity to AQP1 in the divalent block, though with differences in Ba<sup>2+</sup> and Ca<sup>2+</sup> interactions (101).

Given the wealth of structural information for both AQP1 and SoPIP2;1 indicating that the water pore does not allow the passage of cations or protons (184, 188, 216) (but see the discussion of AQP6 above), the favored pathway for ion conductance through AQP1 is via the central pore (33, 232). The differential block by AqB011 of cation conductance but not water permeability through AQP1 supports the idea that the two permeation pathways are physically separate (102). A similar conclusion was based on pCMBS inhibition of water but not ion permeation (175). Mutations of residues lining the central pore also change the ion conductance characteristics of AQP1 (33). The central pore of AQP1, SoPIP2;1, and, by homology, AtPIP2;1 is lined by TM2 and TM5 helices of each monomer (18, 228) (**Figure 3c**) and has general similarity across all AQPs with a large central cavity and a highly conserved constriction at the extracellular side (178). There is also a prominent constriction on the cytoplasmic side that is highly conserved among AQPs formed by hydrophobic side chains of Leu200 (AtPIP2;1), L205 (SoPIP2;1), and L170 (AQP1) on the cytosolic end of H5 bordered by two prolines in PIP2s with the motif PLP (**Figures 2a** and **4**). Hypothetically, this could form a hinge, noting its proximity to loop D, that can gate the central pore as in the PVP hinge in H6 of voltage-gated K<sup>+</sup> channels (173). L170 of AQP1 along with four other barrier residues mutated to alanine resulted in increased permeation for TEA<sup>+</sup> (33). Mutations in H2 and H5 also affect the formation of tetramers in PIP2;1 (228).

Constrictions in the central pore are different between AQP1, SoPIP2;1, AtPIP2;4, and AtPIP2;1 (based on SWISS-MODEL homology model P43286 using AtPIP2;4 as a template), with the PIPs having another constriction at the extracellular side formed by the four Cys residues of loop A, not present in AQP1, that form a disulfide link between the two monomers common to all PIPs (22). This is thought to stabilize the tetramer, but mutants show no differences in water transport, membrane targeting, or tetramer formation (22). Ion conductance of these mutants has not been reported. Loop A has been implicated in heterotetramer organization (92). Interestingly, there are four side pores from the central pore to the extracellular vestibule of each monomer, with the four Cys residues of loop A forming a cap over the entrance to the central pore. The net negative charge of loop A in AtPIP2;1 is quite prominent, and its larger size is the main difference between PIP2;1/PIP2;2 and the other PIP2s including AtPIP2;7, which does not show ion transport. These negatively charged residues may be implicated in the extracellular divalent sensitivity that differs between PIP2;1, PIP2;2, and AQP1 (101).

The generally hydrophobic interior of the central pore would require an opening sufficient to allow a hydrated ion to permeate (232). An MD simulation of AQP1 was facilitated by starting

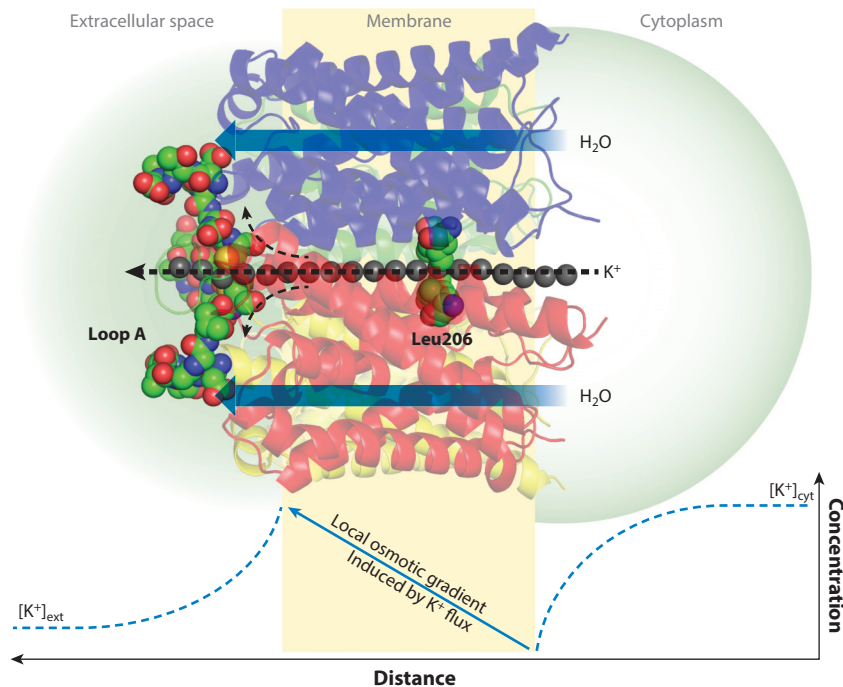


**Figure 4**

Hypothetical water-ion coupling via AtPIP2;1.  $K^+$  (or  $Na^+$ ) flux via the central pore could establish a local osmotic gradient via a transport number effect (10) that would provide the driving force for water flow through the four intrasubunit pores, even though the bulk concentration gradient would not support an osmotic flow. This is distinct from electroosmosis or ion coupling with water through the same pore (e.g., 80). Green shading indicates a possible ion concentration gradient in the unstirred layer induced by the flux of  $K^+$ . Water flow under an osmotic gradient would also influence the ion gradients for conduction via the central pore. Also shown are the two constriction regions in the central pore (Leu206) and loop A for each monomer with negatively charged Asp residues. The gray spheres in the central pore do not represent  $K^+$  ions; rather, they represent the trajectory through the central pore. The structure is a homology model of AtPIP2;1 modeled on AtPIP2;4 (PDB ID 6qim) (206). Structure obtained from SWISS-MODEL P43286; figure adapted from images created with PyMOL.

with a  $Na^+$  ion in the pore, which accelerated water molecules to ingress and create a pathway for  $Na^+$  ions subsequently to permeate with hydration shells (118). This was associated with a large change in the conformation of loop D (232). Another MD with AQP4 simulated electroporation and the subsequent conduction of  $Cl^-$  and  $Na^+$  ions via the central and intrasubunit pores (16). These events required large initial electric fields that would be nonphysiological, and AQP4 is not known to form ion channels in heterologous systems. Noting that ion conductance through AQP1 and AtPIP2;1/AtPIP2;2 is not voltage dependent, neither a large negative nor positive voltage is required to precondition ion conductance.

As for the above discussion of OsPIP1;3, the ion-conducting PIP2s (icPIP2s) may not form exclusive homotetramers in the plasma membrane, though evidence has been presented for exclusive homotetramers of spinach SoPIP2;1 and a PIP1 (56). When coexpressed with HvPIP1 members in *Xenopus* oocytes, the ion conductance of HvPIP2;8 is greatly reduced but not necessarily abolished for certain HvPIP1 combinations with HvPIP2;8 (190). The frequency and variation of PIP2/PIP1 heterotetramers in planta remain important questions not only for the

regulation of ion conductance but also for the regulation of water conductance (222, 223). Interestingly, there is also an inverse relationship in water:ion selectivity with presumed heterotetramers of PIP1:PIP2 (when coexpressed in *Xenopus*), reducing ion conductance and increasing water conductance.

**A mutually exclusive gating hypothesis.** The structures of SoPIP2;1 solved for the open and closed states of the intrasubunit pore (188) may give some clues about possible gating in the central pore. The central pore of biological assemblies of SoPIP2;1 shows interesting differences in restriction sites between the open and closed states of the intrasubunit pore, keeping in mind the apparent reciprocity of water and ion transport revealed by the phosphorylation-mimic mutants (158, 190) (**Figure 3a**). When intrasubunit pores are open, the constriction has a small diameter at Leu205 and a kink in the central pore; this may suggest a closed state. When the intrasubunit pores are closed [when Cd<sup>+</sup> stabilized (188) or in some phosphomimic mutants (138)] with loop D twisted over the top of the respective water pore and plugging the intrasubunit pore with Leu197 (188), this twists H5 (188) to expand the Leu205 constriction, opening an iris-like diaphragm (**Figure 3c,d**). The result is a wider opening to the central pore, seemingly wide enough for the entry of a water molecule. It is interesting to note that the monovalent cation selectivity series obtained for AQP1, which is likely similar to that of AtPIP2;1 (i.e., K<sup>+</sup> > Na<sup>+</sup>), would suggest a minimum pore radius of less than 2 Å (106) if molecular sieving was solely responsible for selectivity and if the ions were dehydrated in transit, which seems unlikely in AQPs lacking the classic K<sup>+</sup> channel selectivity filter sequence. However, K<sup>+</sup> ions may permeate through pores with diameters >2.4 Å with distorted hydration shells (164). There are several ion channels that have hydrophobic regions in the pore with similar diameters to those observed in the icAQPs, and these have been proposed to show the phenomenon of hydrophobic gating (7, 159). The bacterial CmTMEM175 K<sup>+</sup> channel (PDB ID 5VRE), a homolog of the lysosomal K<sup>+</sup> channel in eukaryotes (not in plants), is formed by a tetramer of monomers of 6-TM helices with the central pore containing hydrophobic leucine constrictions (108). The central pore of the bacterial MtTMEM175 (PDB ID 6HD8) is proposed to open through a rotation of helix 1 in “iris-like motions” (31). This removes the leucine constriction gate and exposes the proposed K<sup>+</sup> selectivity filter consisting of threonine residues. Additional serine residues in an outer vestibule also impart K<sup>+</sup> selectivity. This proposed combined gating and selectivity mechanism may be relevant to the icPIP2s since there are also similarities in cation transport (31).

A simple gating model is proposed in **Figure 3b** to account for the inverse relationship observed between ion and water conductance in AtPIP2;1. It is based on the open and closed structures of SoPIP2;1 and the assumption that each intrasubunit (monomer) water pore gates independently. If all four monomer pores have to close before the central tetramer pore can be primed for opening, a relationship can be obtained between the  $P_{\text{open}}$  of the monomer (water) pore ( $P_{m_{\text{open}}}$ ) and the  $P_{\text{open}}$  of the tetrameric central (ion) pore ( $P_{t_{\text{open}}}$ ) (expression in **Figure 3a**). Surprisingly, this simple model fits the data of Reference 158 reasonably well. It is also possible that cooperativity between the gating of each intrasubunit pore will affect the central pore. However, the differences seen in the central pore of the biological assemblies of SoPIP2;1, shown in **Figure 3** in the open and closed states, must be taken with caution since the resolutions and crystal conformations of the two structures are very different and may not allow the interpretation we take in support of this hypothesis. Nevertheless, the movement and half turn of TM5 during the gating of the intrasubunit pore (188) (**Figure 2**) may be expected to alter the central pore diameter in some regions and to expose polar side chains to the pore lumen, which is conducive of ion conduction. Also, the movement of TM1 (138) may affect the orientation of LA that caps the external entrance to the central pore.

---

**Intrasubunit pore:**  
a pore within the monomer or subunit of an aquaporin tetramer

---

**Can ion and water flow be coupled?** In the case of water and monovalent cations for AtPIP2;1, it would seem that these could be mutually exclusive (156, 158). However, when dealing with a population of channels in a cell membrane, it is difficult to exclude the possibility that a state can exist where ions and water can permeate at the same time. Based on the gating hypothesis above, this would not happen at the single channel level, though rapid switching of the subunit pore from open for water in each monomer (with the central pore closed for cations) to closed for all subunit pores (with the central pore open for cations) could result in a local coupling between water and ions via a transport number effect (10), as opposed to electroosmosis (11, 78, 80) (**Figure 4**).

It is important here to consider quantitatively the transport rates for ions and water through the single tetramer to test the feasibility of this type of coupling. We can estimate the open probability of the ion channel (i.e., the tetrameric central pore) ( $P_{t_{open}}$ ) of AtPIP2;1 by making a few assumptions and basing it on the knowledge that total membrane conductance is equal to the *number of channels* ( $n$ )  $\times$  *channel open probability* ( $P_{t_{open}}$ )  $\times$  *unitary-channel ion conductance* (4). First we assume that the unitary channel ion conductance of PIP2;1 is similar to that of AQP1 [though the measured values range widely from 2 to 10 (175) to over 100 pS (6)]. The AtPIP2;1 S283D mutant expressed in *Xenopus* oocytes gave a membrane conductance of 100  $\mu$ S (158) that we assume is near to its maximum ion channel activation. This would give  $n \times P_{t_{open}}$  in the oocyte membrane as:

$$n \times P_{t_{open}} = 100 \times 10^{-6} / 100 \times 10^{-12} (\text{for } 100 \text{ pS channel}) = 10^6, \text{ or } 10^7 \text{ for } 10 \text{ pS channel.}$$

To estimate  $n$  we use the water permeability measurements of AtPIP2;1. The average maximum osmotic water permeability ( $P_{os}$ ) for an oocyte expressing wild-type AtPIP2;1 is  $1 \times 10^{-3} \text{ cm s}^{-1}$ , using actual oocyte surface area (36). If the unitary water permeability of an AtPIP2;1 intrasubunit pore is about  $4 \times 10^{-13} \text{ cm}^3 \text{ s}^{-1}$  as per AQP1 (28, 80), this would mean that an approximate AtPIP2;1 tetramer density in the oocyte membrane is  $6 \times 10^8 \text{ cm}^{-2}$ . An average oocyte membrane area of  $0.5 \text{ cm}^2$  per oocyte then gives  $3 \times 10^8$  tetramers/oocyte. Therefore,  $P_{t_{open}} \approx 3 \times 10^{-3}$  (100 pS channel) or  $3 \times 10^{-2}$  (10 pS) or between 0.3 and 3.0%, which is rather low but not so unlikely when the total number of channels is used to infer  $P_{t_{open}}$  rather than the electrically active channels observed in patch clamp (26). It should be noted for the above approximation that AQPs may show a wide range of unitary water permeability (80), and unstirred layers may result in the  $P_{os}$  of oocytes being underestimated (28).

The gating model (**Figure 3a**) would predict that the open probability of the monomer (water) pore ( $P_{m_{open}}$ ) becomes quite low (0.015) before  $P_{t_{open}}$  starts to approach 0.5, perhaps precluding ion:water coupling. At  $P_{t_{open}}$  of 0.5, the open ion channel conductance would have to be very low ( $\sim 0.1$  pS) to account for the whole-cell ion conductance. To account for the higher single-channel conductance measured for AQP1, it would seem that the  $P_{t_{open}}$  is low. This is perhaps accounted for by a silent mode, as shown in **Figure 3**, that may be primed for hydrophobic gating (7).

AQPs are at a very high density in the membrane, and they have a large impact on water permeability. If every AQP were conducting ions simultaneously, it would be catastrophic for the cell. This could only occur if the single-channel conductance of the ion pore was very low or had a very low  $P_{open}$ . Ion coupling could occur if the tetramers formed clusters in microdomains or rafts (117) so that in a given cluster there may be one or two ion channels active with many more water channels. It does raise the question why evolution has arrived at a water and ion channel combined in the one structure, noting that some  $\text{K}^+$  channels can have high water permeability (e.g., bacterial KcsA) (80), and we cannot exclude the possibility that a state can occur in PIP2 icAQPs where both water and ions can conduct at the same time (**Figures 3b** and **4**).

For water to be pumped against an osmotic gradient, AQPs would have to be closed to prevent a futile cycle back down the gradient (160, 211, 212). Based on the model proposed in **Figure 3**

to explain the inverse water and ion permeation in Reference 158, this closure of the water channel would correspond to the opening of an ion channel permeable to  $K^+$  (and  $Na^+$ ). This may facilitate water pumping by allowing the cycling of  $K^+$ , if  $K^+$  is the driver ion for water transport through another transporter (see, e.g., 234) and coupled to an electrochemical gradient generated by the proton pump (211, 212). The energy required to pump water is very dependent on the back leak via AQPs such that it would only be feasible if AQPs were substantially shut (59, figure 8); such a model would not be consistent with parallel osmotically driven water fluxes (160). Further consideration of the energetics of water pumping as per Raven & Doblin (160) and Wegner (211, 212) need to be assessed in the light of the recent discoveries of inverse ion/water gating of PIP2s. It has also been speculated that water flow through an AQP could generate energy akin to a turbine (59). In a general sense, the ion channel activity of AtPIP2;1, AtPIP2;2, and HvPIP2;8 may present a mechanism for this based on the inverse gating and the link between water transport and electrogenic cation transport. Coupling between ion and water flow is predicted to reduce the apparent water permeability that is observed when ion conductance becomes larger (**Figure 3a**). It is unknown whether the gradient for water transport can be coupled to the gating of the ion channel in the tetramer, though there is evidence that pressure gradients and osmotic gradients can gate plant AQPs (204, 227).

### AtPIP2;1: A Multifunctional Conditional System with a Large Permissive Permeability Range

Proposed functions of AtPIP2;1 and AtPIP2;2 and orthologs range from highly regulated roles in water transport in leaves (95, 151, 152, 157), roots (35, 47, 88, 153), and guard cells (66), to  $H_2O_2$  signaling in guard cells (167), cell-to-cell transport of systemic signals (53),  $CO_2$  sensing in guard cells (205), growth responses to drought stress (236), and water transport regulation in response to salinity (97) (**Figure 5**). The role of PIP2s in guard cell closure (66, 167, 205) is complicated by the observation that a quadruple *Arabidopsis* mutant (*pip1;1 pip1;2 pip2;2 pip2;1*) did not affect closure rates in response to abscisic acid compared to wild type (34). The interaction between *Camelina sativa* CsPIP2;1 and the hydrophobic Rare Cold Inducible proteins (CsRCI2E, CsRCI2F) induced by salinity reduces the membrane abundance and water transport of CsPIP2;1 when expressed in *Xenopus* oocytes (97). This is interesting since these proteins have been linked to regulating membrane potential by reducing membrane hyperpolarization, which would reduce the gradient for nonselective cation influx; thus, there is a protective effect under salinity (96). This link is not consistent with water transport but is entirely consistent with nonselective cation transport via CsPIP2;1.

The large array of protein interactions and PTMs associated with AtPIP2;1 and other AQPs may indicate that how a transporter is placed for a particular function is dictated by what substrates are transported at its location, the proteins that interact, and the associated PTMs (57). This would be context dependent, i.e., dependent on development gradients, response to biotic and abiotic stress, and time (**Figure 5**). The fact that so many different proteins can interact with AtPIP2;1 (15), some of which have been shown to affect function (35, 152), combined with diverse possible combinations of phosphorylations by different kinases (66, 181, 217, 218), indicates a multifunctional combinatorial system with potential permeabilities spanning a broad range of substrates, i.e., from cations to  $CO_2$ . Permeabilities of lipid membranes are in the range of  $10^{-14}$ – $10^{-12}$   $m\ s^{-1}$  for ions,  $10^{-4}$   $m\ s^{-1}$  for water, and upwards of  $1\ m\ s^{-1}$  for  $CO_2$  (72). Thus, some AQPs have the potential to influence membrane permeability over a range spanning from 12 to 14 orders of magnitude, among the greatest of any known types of transporters.

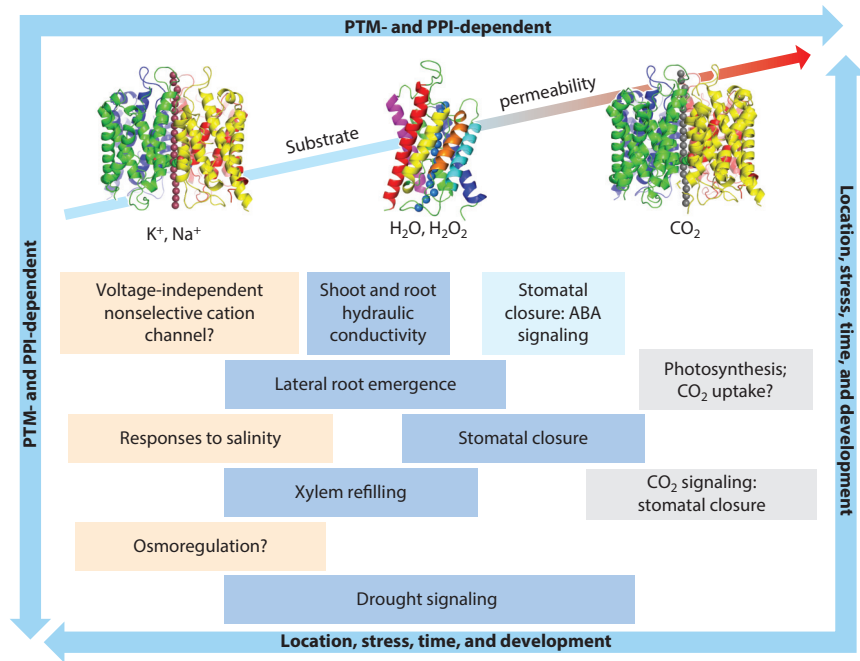


**Figure 5**

Multidimensional functionality of AtPIP2;1, which is able to transport cations, water, H<sub>2</sub>O<sub>2</sub>, and CO<sub>2</sub> and is dependent on PTMs and/or PPIs. The various known functions and putative functions are indicated under each transport mode. It is not known if simultaneous transport of different substrates can occur, but this might be relevant to some functions (e.g., signaling) via ion conductance and/or H<sub>2</sub>O<sub>2</sub> permeability. Structures indicated are for AtPIP2;1 modeled on AtPIP2;4 (PDB ID 6qim) (206). Structure obtained from SWISS-MODEL P43286. Also shown (*spheres of different colors*) are the possible pathways for cation (*left*) and/or CO<sub>2</sub> (*right*) movement through the central pore of the tetramer and H<sub>2</sub>O and/or H<sub>2</sub>O<sub>2</sub> through the intrasubunit pore (water pore). Data obtained from PoreWalker (145) and drawn with PyMOL with a cutaway view to make the pores more visible. Abbreviations: ABA, abscisic acid; PPI, protein-protein interaction; PTM, posttranslational modification.

## FUTURE PERSPECTIVES ON THE DISCOVERY OF PLANT ION-CONDUCTING AQUAPORINS AND THEIR ROLES

Currently, there are only a handful of examples of icAQPs in plants (**Figure 1**), and some of these are somewhat speculative (TIP2;1, VvXIP1); all require further confirmation with different systems and in planta function. However, the implications of icAQPs are sufficiently important that further surveys of each of the members of the subfamilies should be carried out, and we should no longer assume that AQPs are only permeable to neutral solutes. AQP permeability surveys are complicated by the likelihood that PTMs and PPIs can modify or switch off ion conductance and that the systems selected for the analyses could influence the observed outcomes. For example, in analyses of neutral solute selectivity, AQP ion-conducting states could alter measurements of permeability to water or other neutral solutes, such as CO<sub>2</sub> and NH<sub>3</sub> that have ionic counterparts. The roles of icAQPs in planta have not been determined, and resolving this will be challenging given the multifunctional roles already reported for some AQPs, especially AtPIP2;1. Redundancy (e.g., AtPIP2;1 and AtPIP2;2) and secondary effects related to water transport regulation (**Figure 5**) will also impact ion fluxes (134) when mutants are assessed.

More crystal structures of plant AQPs in various functional states could facilitate the definition of predictive motifs for icAQPs, which would be useful for identifying new icAQP candidates and distinguishing whether ions move through intrasubunit or central pore pathways. Initial attempts to find key structural determinants of ion transport through PIP2s have yielded candidate sites for mutational studies of LD and C-terminal domains, loop A for possible divalent sensitivity, and the PLP motif and threonine residues in H5 (31) for ion channel gating/selectivity, but much remains unknown compared with the advanced structural features used to predict water and neutral molecule permeation via the intrasubunit pores (e.g., 80, 99, 120). Structure–function exploration through MD simulations would greatly facilitate the understanding of the ion transport features of icAQPs.

The possible coupling between water and ion flows has been speculated upon in relation to water pumping and energy generation (59, 213). The movement of water into the xylem sometimes against an apparent water potential gradient could be explained by such coupling (211, 212). The PIP2;1/PIP2;2 proteins provide a possible component for such a mechanism, but detailed studies of how the ion channel is gated in relation to water flow will be required. The opportunity to manipulate icAQP function will open avenues to better understand the relationships between water and ion flows in plants.

The multifunctionality of some plant AQPs (e.g., AtPIP2;1) is likely due in part to the range of PTMs and PPIs and reinforces the unique position that AQPs occupy in the transportomes of plants. That AtPIP2;1 is one of the most studied AQPs could also indicate that when further information is obtained on some of the other AQPs, such as OsPIP1;3 and TIP2;1, similar multifunctionality will be revealed.

---

**C-terminal domain:**  
carboxyl terminal  
domain of a protein

---

## SUMMARY POINTS

1. There are aquaporins (AQPs) in plants that have been shown to carry either univalent cations or anions electrogenically [ion-conducting AQPs (icAQPs)] when expressed in heterologous systems or lipid bilayers. There are analogous icAQPs in animal cells.
2. The cation conducting icPIP2s from different species can show different selectivity, i.e.,  $K^+ > Na^+$  or  $Na^+ > K^+$ , and different sensitivity to blocking by divalent cations.
3. Different icAQPs may account for several so far unidentified (genetically) nonselective ion channels in the plasma membrane, vacuolar membrane, and legume symbiosome membrane.
4. Phosphorylation of PIP2 AQPs at certain sites appears to regulate the ion conductance in an inverse manner to water permeability.
5. Water may be coupled to ion flow in icAQPs depending on the way the ion- and water-conducting pathways are gated, but it is likely that only a small proportion of icAQPs in a cell will be in an ion-conducting state at any given time.
6. Some AQPs, e.g., AtPIP2;1, have a wide range of solute permeability (univalent cations,  $H_2O$ ,  $H_2O_2$ ,  $CO_2$ ) and could be considered as multifunctional conditional transport systems. This requires tight regulation most probably linked to posttranslational modifications and protein–protein interactions.
7. Defining AQPs as gated ion channels in addition to neutral solute pores opens new paradigms for modeling cellular regulation of fluid movement and volume control.

8. An open-minded reanalysis of broad classes of AQPs previously assumed to be purely water-selective channels should consider signaling pathways that might be required for gating.

## DISCLOSURE STATEMENT

The authors are not aware of any affiliations, memberships, funding, or financial holdings that might be perceived as affecting the objectivity of this review.

## ACKNOWLEDGMENTS

We thank David Day for initial comments on the manuscript. The work of the authors is supported by the Australian Research Council (CE140100008 and DP190102725 to S.D.T., S.A.M., C.S.B., and J.Q.; DP190102725 and DP190101745 to A.J.Y.; CE1401000015 to C.S.B. and S.A.M.; and FT180100476 to C.S.B.).

## LITERATURE CITED

1. Agre P, Lee MD, Devidas S, Guggino WB. 1997. Aquaporins and ion conductance. *Science* 275:1490–92
2. Ahmed J, Merx S, Boutry M, Chaumont F. 2020. Evolutionary and predictive functional insights into the aquaporin gene family in the allotetraploid plant *Nicotiana tabacum*. *Int. J. Mol. Sci.* 21:4743
3. Alishahi M, Kamali R. 2019. A novel molecular dynamics study of CO<sub>2</sub> permeation through aquaporin-5. *Eur. Phys. J. E* 42:151
4. Alvarez O, Gonzalez C, Latorre R. 2002. Counting channels: a tutorial guide on ion channel fluctuation analysis. *Adv. Physiol. Educ.* 26:327–41
5. Amodeo G, Sutka M, Dorr R, Parisi M. 2002. Protoplasmic pH modifies water and solute transfer in *Beta vulgaris* root vacuoles. *J. Membr. Biol.* 187:175–84
6. Anthony TL, Brooks HL, Boassa D, Leonov S, Yanocho GM, et al. 2000. Cloned human aquaporin-1 is a cyclic GMP-gated ion channel. *Mol. Pharmacol.* 57:576–88
7. Aryal P, Sansom MSP, Tucker SJ. 2015. Hydrophobic gating in ion channels. *J. Mol. Biol.* 427:121–30
8. Azad AK, Ahmed J, Alum MA, Hasan MM, Ishikawa T, et al. 2016. Genome-wide characterization of major intrinsic proteins in four grass plants and their non-aqua transport selectivity profiles with comparative perspective. *PLOS ONE* 11:e0157735
9. Barbier-Brygoo H, De Angeli A, Filleur S, Frachisse JM, Gambale F, et al. 2011. Anion channels/transporters in plants: from molecular bases to regulatory networks. *Annu. Rev. Plant Biol.* 62:25–51
10. Barry PH. 1998. Derivation of unstirred-layer transport number equations from the Nernst-Planck flux equations. *Biophys. J.* 74:2903–5
11. Barry PH, Hope AB. 1969. Electro-osmosis in *Chara* and *Nitella* cells. *Biochim. Biophys. Acta Biomembr.* 193:124–28
12. Battle AR, Ridone P, Bavi N, Nakayama Y, Nikolaev YA, Martinac B. 2015. Lipid-protein interactions: lessons learned from stress. *Biochim. Biophys. Acta Biomembr.* 1848:1744–56
13. Beitz E, Liu K, Ikeda M, Guggino WB, Agre P, Yasui M. 2006. Determinants of AQP6 trafficking to intracellular sites versus the plasma membrane in transfected mammalian cells. *Biol. Cell* 98:101–9
14. Beitz E, Wu BH, Holm LM, Schultz JE, Zeuthen T. 2006. Point mutations in the aromatic/arginine region in aquaporin 1 allow passage of urea, glycerol, ammonia, and protons. *PNAS* 103:269–74
15. Bellati J, Champeyroux C, Hem S, Rofidal V, Krouk G, et al. 2016. Novel aquaporin regulatory mechanisms revealed by interactomics. *Mol. Cell. Proteom.* 15:3473–87

---

15. Shows that hundreds of proteins can interact with AtPIP2;1, and two key kinases could regulate AtPIP2;1 water transport.

---

16. Bernardi M, Marracino P, Liberti M, Gárate JA, Burnham CJ, et al. 2019. Controlling ionic conductivity through transprotein electropores in human aquaporin 4: a non-equilibrium molecular-dynamics study. *Phys. Chem. Chem. Phys.* 21:3339–46
17. Bernareggi A, Conte G, Constanti A, Borelli V, Vita F, Zabucchi G. 2019. On the mechanism of the electrophysiological changes and membrane lesions induced by asbestos fiber exposure in *Xenopus laevis* oocytes. *Sci. Rep.* 9:2014
18. Berny MC, Gilis D, Rooman M, Chaumont F. 2016. Single mutations in the transmembrane domains of maize plasma membrane aquaporins affect the activity of monomers within a heterotetramer. *Mol. Plant* 9:986–1003
19. Besserer A, Burnotte E, Bienert GP, Chevalier AS, Errachid A, et al. 2012. Selective regulation of maize plasma membrane aquaporin trafficking and activity by the SNARE SYP121. *Plant Cell* 24:3463–81
20. Bezerra-Neto JP, de Araujo FC, Ferreira-Neto JRC, da Silva MD, Pandolfi V, et al. 2019. Plant aquaporins: diversity, evolution and biotechnological applications. *Curr. Protein Pept. Sci.* 20:368–95
21. Bienert GP, Bienert MD, Jahn TP, Boutry M, Chaumont F. 2011. *Solanaceae* XIPs are plasma membrane aquaporins that facilitate the transport of many uncharged substrates. *Plant J.* 66:306–17
22. Bienert GP, Cavez D, Besserer A, Berny MC, Gilis D, et al. 2012. A conserved cysteine residue is involved in disulfide bond formation between plant plasma membrane aquaporin monomers. *Biochem. J.* 445:101–11
23. Bienert GP, Chaumont F. 2014. Aquaporin-facilitated transmembrane diffusion of hydrogen peroxide. *Biochim. Biophys. Acta Gen. Subj.* 1840:1596–604
24. Bienert GP, Moller ALB, Kristiansen KA, Schulz A, Moller IM, et al. 2007. Specific aquaporins facilitate the diffusion of hydrogen peroxide across membranes. *J. Biol. Chem.* 282:1183–92
25. Bienert MD, Diehn TA, Richet N, Chaumont F, Bienert GP. 2018. Heterotetramerization of plant PIP1 and PIP2 aquaporins is an evolutionary ancient feature to guide PIP1 plasma membrane localization and function. *Front. Plant Sci.* 9:382
26. Boassa D, Stamer WD, Yool AJ. 2006. Ion channel function of aquaporin-1 natively expressed in choroid plexus. *J. Neurosci.* 26:7811–19
27. Borgnia M, Nielsen S, Engel A, Agre P. 1999. Cellular and molecular biology of the aquaporin water channels. *Annu. Rev. Biochem.* 68:425–58
28. Boytsov D, Hanneschlaeger C, Horner A, Siligan C, Pohl P. 2020. Micropipette aspiration-based assessment of single channel water permeability. *Biotechnol. J.* 15:1900450
29. Bruggemann LI, Pottosin II, Schonknecht G. 1999. Cytoplasmic magnesium regulates the fast activating vacuolar cation channel. *J. Exp. Bot.* 50:1547–52
30. Bruggemann LI, Pottosin II, Schonknecht G. 1999. Selectivity of the fast activating vacuolar cation channel. *J. Exp. Bot.* 50:873–76
31. Brunner JD, Jakob RP, Schulze T, Neldner Y, Moroni A, et al. 2020. Structural basis for ion selectivity in TMEM175 K<sup>+</sup> channels. *eLife* 9:e53683
32. **Byrt CS, Zhao M, Kourghi M, Bose J, Henderson SW, et al. 2017. Non-selective cation channel activity of aquaporin AtPIP2;1 regulated by Ca<sup>2+</sup> and pH. *Plant Cell Environ.* 40:802–15**
33. Campbell EM, Birdsell DN, Yool AJ. 2012. The activity of human aquaporin 1 as a cGMP-gated cation channel is regulated by tyrosine phosphorylation in the carboxyl-terminal domain. *Mol. Pharmacol.* 81:97–105
34. Ceciliato PHO, Zhang J, Liu Q, Shen X, Hu HH, et al. 2019. Intact leaf gas exchange provides a robust method for measuring the kinetics of stomatal conductance responses to abscisic acid and other small molecules in *Arabidopsis* and grasses. *Plant Methods* 15:38
35. Champeyroux C, Bellati J, Barberon M, Rofidal V, Maurel C, Santoni V. 2019. Regulation of a plant aquaporin by a Casparian strip membrane domain protein-like. *Plant Cell Environ.* 42:1788–801
36. Chandy G, Zampighi GA, Kremann M, Hall JE. 1997. Comparison of the water transporting properties of MIP and AQP1. *J. Membr. Biol.* 159:29–39
37. Chaumont F, Tyerman SD. 2014. Aquaporins: highly regulated channels controlling plant water relations. *Plant Physiol.* 164:1600–18
38. Choi WG, Roberts DM. 2007. *Arabidopsis* NIP2;1, a major intrinsic protein transporter of lactic acid induced by anoxic stress. *J. Biol. Chem.* 282:24209–18

---

32. Finds that AtPIP2;1 induced nonselective univalent cation conductance, which was inhibited by low pH and external Ca<sup>2+</sup>.

---

39. Clarke VC, Loughlin PC, Day DA, Smith PMC. 2014. Transport processes of the legume symbiosome membrane. *Front. Plant Sci.* 5:699
40. Danielson JÅH, Johanson U. 2008. Unexpected complexity of the Aquaporin gene family in the moss *Physcomitrella patens*. *BMC Plant Biol.* 8:45
41. De Ieso ML, Pei JV, Nourmohammadi S, Smith E, Chow PH, et al. 2019. Combined pharmacological administration of AQP1 ion channel blocker AqB011 and water channel blocker Bacopaside II amplifies inhibition of colon cancer cell migration. *Sci. Rep.* 9:12635
42. De Rosa A, Watson-Lazowski A, Evans JR, Groszmann M. 2020. Genome-wide identification and characterisation of Aquaporins in *Nicotiana tabacum* and their relationships with other Solanaceae species. *BMC Plant Biol.* 20:266
43. Dean RM, Rivers RL, Zeidel ML, Roberts DM. 1999. Purification and functional reconstitution of soybean nodulin 26. An aquaporin with water and glycerol transport properties. *Biochemistry* 38:347–53
44. Demidchik V, Tester M. 2002. Sodium fluxes through nonselective cation channels in the plasma membrane of protoplasts from Arabidopsis roots. *Plant Physiol.* 128:379–87
45. Di Pietro M, Vialaret J, Li G-W, Hem S, Prado K, et al. 2013. Coordinated post-translational responses of aquaporins to abiotic and nutritional stimuli in *Arabidopsis* roots. *Mol. Cell. Proteom.* 12:3886–97
46. Ding L, Chaumont F. 2020. Are aquaporins expressed in stomatal complexes promising targets to enhance stomatal dynamics? *Front. Plant Sci.* 11:458
47. Ding L, Uehlein N, Kaldenhoff R, Guo SW, Zhu YY, Kai L. 2019. Aquaporin *PIP2;1* affects water transport and root growth in rice (*Oryza sativa* L.). *Plant Physiol. Biochem.* 139:152–60
48. Dynowski M, Schaaf G, Loque D, Moran O, Ludewig U. 2008. Plant plasma membrane water channels conduct the signalling molecule H<sub>2</sub>O<sub>2</sub>. *Biochem. J.* 414:53–61
49. Ebihara L. 1996. *Xenopus* Connexin38 forms hemi-gap-junctional channels in the nonjunctional plasma membrane of *Xenopus* oocytes. *Biophys. J.* 71:742–48
50. Eisenberg D, Gill HS, Pfluegl GMU, Rotstein SH. 2000. Structure–function relationships of glutamine synthetases. *Biochim. Biophys. Acta Protein Struct. Molec. Enzym.* 1477:122–45
51. Essah PA, Davenport R, Tester M. 2003. Sodium influx and accumulation in Arabidopsis. *Plant Physiol.* 133:307–18
52. Fetter K, Van Wilder V, Moshelion M, Chaumont F. 2004. Interactions between plasma membrane aquaporins modulate their water channel activity. *Plant Cell* 16:215–28
53. Fichman Y, Myers RJ Jr., Grant DG, Mittler R. 2020. Plasmodesmata-localized proteins and reactive oxygen species orchestrate light-induced rapid systemic signaling in *Arabidopsis*. bioRxiv 2020.10.07.329995. <https://doi.org/10.1101/2020.10.07.329995>
54. Fortin MG, Morrison NA, Verma DPS. 1987. Nodulin-26, a peribacteroid membrane nodulin is expressed independently of the development of the peribacteroid compartment. *Nucleic Acids Res.* 15:813–24
55. Fortuna AC, De Palma GZ, Car LA, Armentia L, Vitali V, et al. 2019. Gating in plant plasma membrane aquaporins: the involvement of leucine in the formation of a pore constriction in the closed state. *FEBS J.* 286:3473–87
56. Fotiadis D, Jenö P, Mini T, Wirtz S, Müller SA, et al. 2001. Structural characterization of two aquaporins isolated from native spinach leaf plasma membranes. *J. Biol. Chem.* 276:1707–14
57. Fox AR, Maistriaux LC, Chaumont F. 2017. Toward understanding of the high number of plant aquaporin isoforms and multiple regulation mechanisms. *Plant Sci.* 264:179–87
58. Frick A, Jarva M, Tornroth-Horsefield S. 2013. Structural basis for pH gating of plant aquaporins. *FEBS Lett.* 587:989–93
59. Fricke W. 2017. Water transport and energy. *Plant Cell Environ.* 40:977–94
60. Fu DX, Libson A, Miercke LJW, Weitzman C, Nollert P, et al. 2000. Structure of a glycerol-conducting channel and the basis for its selectivity. *Science* 290:481–86
61. Gazzarrini S, Kang M, Epimashko S, Van Etten JL, Dainty J, et al. 2006. *Chlorella* virus MT325 encodes water and potassium channels that interact synergistically. *PNAS* 103:5355–60
62. Gloser V, Zwieniecki MA, Orians CM, Holbrook NM. 2007. Dynamic changes in root hydraulic properties in response to nitrate availability. *J. Exp. Bot.* 58:2409–15

63. Gonen T, Walz T. 2006. The structure of aquaporins. *Q. Rev. Biophys.* 39:361–96
64. Grefen C, Karnik R, Larson E, Lefoulon C, Wang YZ, et al. 2015. A vesicle-trafficking protein commandeers Kv channel voltage sensors for voltage-dependent secretion. *Nat. Plants* 1:15108
65. Grondin A, Mauleon R, Vadez V, Henry A. 2016. Root aquaporins contribute to whole plant water fluxes under drought stress in rice (*Oryza sativa* L.). *Plant Cell Environ.* 39:347–65
66. Grondin A, Rodrigues O, Verdoucq L, Merlot S, Leonhardt N, Maurel C. 2015. Aquaporins contribute to ABA-triggered stomatal closure through OST1-mediated phosphorylation. *Plant Cell* 27:1945–54
67. Groszmann M, Osborn HL, Evans JR. 2017. Carbon dioxide and water transport through plant aquaporins. *Plant Cell Environ.* 40:938–61
68. Guenther JF, Chanmanivone N, Galetovic MP, Wallace IS, Cobb JA, Roberts DM. 2003. Phosphorylation of soybean nodulin 26 on serine 262 enhances water permeability and is regulated developmentally and by osmotic signals. *Plant Cell* 15:981–91
69. Guo L, Wang ZY, Lin H, Cui WE, Chen J, et al. 2006. Expression and functional analysis of the rice plasma-membrane intrinsic protein gene family. *Cell Res.* 16:277–86
70. Hachez C, Laloux T, Reinhardt H, Cavez D, Degand H, et al. 2014. *Arabidopsis* SNAREs SYP61 and SYP121 coordinate the trafficking of plasma membrane aquaporin PIP2;7 to modulate the cell membrane water permeability. *Plant Cell* 26:3132–47
71. Hachez C, Veljanovski V, Reinhardt H, Guillaumot D, Vanhee C, et al. 2014. The *Arabidopsis* abiotic stress-induced TSP0-related protein reduces cell-surface expression of the aquaporin PIP2;7 through protein-protein interactions and autophagic degradation. *Plant Cell* 26:4974–90
72. Hanneschlaeger C, Homer A, Pohl P. 2019. Intrinsic membrane permeability to small molecules. *Chem. Rev.* 119:5922–53
73. Haydon MJ, Cobbett CS. 2007. Transporters of ligands for essential metal ions in plants. *New Phytol.* 174:499–506
74. Hazama A, Kozono D, Guggino WB, Agre P, Yasui M. 2002. Ion permeation of AQP6 water channel protein. Single-channel recordings after Hg<sup>2+</sup> activation. *J. Biol. Chem.* 277:29224–30
75. Hedrich R, Neher E. 1987. Cytoplasmic calcium regulates voltage-dependent ion channels in plant vacuoles. *Nature* 329:833–36
76. Hill AE, Shachar-Hill B, Shachar-Hill Y. 2004. What are aquaporins for? *J. Membr. Biol.* 197:1–32
77. Holm LM, Jahn TP, Moller ALB, Schjoerring JK, Ferri D, et al. 2005. NH<sub>3</sub> and NH<sub>4</sub><sup>+</sup> permeability in aquaporin-expressing *Xenopus* oocytes. *Pflügers Arch.* 450:415–28
78. Homblé F, Véry AA. 1992. Coupling of water and potassium ions in K<sup>+</sup> channels of the tonoplast of *Chara*. *Biophys. J.* 63:996–99
79. Hooijmaijers C, Rhee JY, Kwak KJ, Chung GC, Horie T, et al. 2012. Hydrogen peroxide permeability of plasma membrane aquaporins of *Arabidopsis thaliana*. *J. Plant Res.* 125:147–53
80. **Horner A, Pohl P. 2018. Single-file transport of water through membrane channels. *Faraday Discuss.* 209:9–33**
81. Hove RM, Bhava M. 2011. Plant aquaporins with non-aqua functions: deciphering the signature sequences. *Plant Mol. Biol.* 75:413–30
82. Hsu JL, Wang LY, Wang SY, Lin CH, Ho KC, et al. 2009. Functional phosphoproteomic profiling of phosphorylation sites in membrane fractions of salt-stressed *Arabidopsis thaliana*. *Proteome Sci.* 7:42
83. Hwang JH, Ellingson SR, Roberts DM. 2010. Ammonia permeability of the soybean nodulin 26 channel. *FEBS Lett.* 584:4339–43
84. Ikeda M, Beitz E, Kozono D, Guggino WB, Agre P, Yasui M. 2002. Characterization of aquaporin-6 as a nitrate channel in mammalian cells. Requirement of pore-lining residue threonine 63. *J. Biol. Chem.* 277:39873–79
85. Isayenkov SV, Maathuis FJM. 2019. Plant salinity stress: Many unanswered questions remain. *Front. Plant Sci.* 10:80
86. Ishibashi K, Hara S, Kondo S. 2009. Aquaporin water channels in mammals. *Clin. Exp. Nephrol.* 13:107–17
87. Jahn TP, Moller ALB, Zeuthen T, Holm LM, Klaerke DA, et al. 2004. Aquaporin homologues in plants and mammals transport ammonia. *FEBS Lett.* 574:31–36

---

**80. Explains water diffusion through aquaporins, including methods to measure water permeability in different experimental systems.**

---

88. Javot H, Lauvergeat V, Santoni V, Martin-Laurent F, Guclu J, et al. 2003. Role of a single aquaporin isoform in root water uptake. *Plant Cell* 15:509–22
89. Jian FM, Tamai K, Yamaji N, Mitani N, Konishi S, et al. 2006. A silicon transporter in rice. *Nature* 440:688–91
90. Johanson U, Karlsson M, Johansson I, Gustavsson S, Sjovald S, et al. 2001. The complete set of genes encoding major intrinsic proteins in Arabidopsis provides a framework for a new nomenclature for major intrinsic proteins in plants. *Plant Physiol.* 126:1358–69
91. Johansson I, Karlsson M, Shukla VK, Chrispeels MJ, Larsson C, Kjellbom P. 1998. Water transport activity of the plasma membrane aquaporin PM28A is regulated by phosphorylation. *Plant Cell* 10:451–59
92. Jozefkowicz C, Rosi P, Sigaut L, Soto G, Pietrasanta LI, et al. 2013. Loop A is critical for the functional interaction of two *Beta vulgaris* PIP aquaporins. *PLOS ONE* 8:e57993
93. Jung JS, Preston GM, Smith BL, Guggino WB, Agre P. 1994. Molecular-structure of the water channel through aquaporin CHIP. The hourglass model. *J. Biol. Chem.* 269:14648–54
94. Kammerloher W, Fischer U, Piechotka GP, Schäffner AR. 1994. Water channels in the plant plasma membrane cloned by immunoselection from a mammalian expression system. *Plant J.* 6:187–99
95. Kelly G, Sade N, Doron-Faigenboim A, Lerner S, Shatil-Cohen A, et al. 2017. Sugar and hexokinase suppress expression of PIP aquaporins and reduce leaf hydraulics that preserves leaf water potential. *Plant J.* 91:325–39
96. Kim HS, Lee JE, Jang HY, Kwak KJ, Ahn SJ. 2016. *CsRCI2A* and *CsRCI2E* genes show opposite salt sensitivity reaction due to membrane potential control. *Acta Physiol. Plant.* 38:50
97. Kim HS, Park W, Lim HG, Eom S, Lee JH, et al. 2019. NaCl-induced *CsRCI2E* and *CsRCI2F* interact with aquaporin *CsPIP2;1* to reduce water transport in *Camelina sativa* L. *Biochem. Biophys. Res. Commun.* 513:213–18
98. Kim MJ, Han JK. 2002. Hydrogen peroxide-induced current in *Xenopus* oocytes: current characteristics similar to those induced by the removal of extracellular calcium. *Biochem. Pharmacol.* 63:569–76
99. Kirscht A, Kaptan SS, Bienert GP, Chaumont F, Nissen P, et al. 2016. Crystal structure of an ammonia-permeable aquaporin. *PLOS Biol.* 14:e1002411
100. Kourghi M, De Ieso ML, Nourmohammadi S, Pei JV, Yool AJ. 2018. Identification of loop D domain amino acids in the human aquaporin-1 channel involved in activation of the ionic conductance and inhibition by AqB011. *Front. Chem.* 6:142
101. Kourghi M, Nourmohammadi S, Pei JV, Qiu J, McGaughey S, et al. 2017. Divalent cations regulate the ion conductance properties of diverse classes of aquaporins. *Int. J. Mol. Sci.* 18:2323
102. Kourghi M, Pei JXV, De Ieso ML, Flynn G, Yool AJ. 2016. Bumetanide derivatives AqB007 and AqB011 selectively block the aquaporin-1 ion channel conductance and slow cancer cell migration. *Mol. Pharmacol.* 89:133–40
103. Kozono D, Yasui M, King LS, Agre P. 2002. Aquaporin water channels: Atomic structure and molecular dynamics meet clinical medicine. *J. Clin. Invest.* 109:1395–99
104. Kromdijk J, Głowacka K, Long SP. 2020. Photosynthetic efficiency and mesophyll conductance are unaffected in *Arabidopsis thaliana* aquaporin knock-out lines. *J. Exp. Bot.* 71:318–29
105. Kuruma A, Hirayama Y, Hartzell HC. 2000. A hyperpolarization- and acid-activated nonselective cation current in *Xenopus* oocytes. *Am. J. Physiol. Cell Physiol.* 279:C1401–13
106. Laio A, Torre V. 1999. Physical origin of selectivity in ionic channels of biological membranes. *Biophys. J.* 76:129–48
107. Laloux T, Junqueira B, Maistriaux LC, Ahmed J, Jurkiewicz A, Chaumont F. 2018. Plant and mammal aquaporins: same but different. *Int. J. Mol. Sci.* 19:521
108. Lee C, Guo JT, Zeng WZ, Kim S, She J, et al. 2017. The lysosomal potassium channel TMEM175 adopts a novel tetrameric architecture. *Nature* 547:472–75
109. Lee HK, Cho SK, Son O, Xu ZY, Hwang I, Kim WT. 2009. Drought stress-induced Rma1H1, a RING membrane-anchor E3 ubiquitin ligase homolog, regulates aquaporin levels via ubiquitination in transgenic *Arabidopsis* plants. *Plant Cell* 21:622–41

---

99. Resolves AtTIP2;1 structure, revealing the mechanism of NH<sub>3</sub> permeation and a side pore that may allow proton permeation.

---

101. Shows that plant and animal icAQPs differ in sensitivity to blocking of ionic conductance by external divalent cations.

---

110. Lee JW, Zhang Y, Weaver CD, Shomer NH, Louis CF, Roberts DM. 1995. Phosphorylation of Nodulin 26 on Serine 262 affects its voltage-sensitive channel activity in planar lipid bilayers. *J. Biol. Chem.* 270:27051–57
111. Lefoulon C, Waghmare S, Karnik R, Blatt MR. 2018. Gating control and K<sup>+</sup> uptake by the KAT1 K<sup>+</sup> channel leveraged through membrane anchoring of the trafficking protein SYP121. *Plant Cell Environ.* 41:2668–77
112. Leitão L, Prista C, Loureiro-Dias MC, Moura TF, Soveral G. 2014. The grapevine tonoplast aquaporin TIP2;1 is a pressure gated water channel. *Biochem. Biophys. Res. Commun.* 450:289–94
113. Leitao L, Prista C, Moura TF, Loureiro-Dias MC, Soveral G. 2012. Grapevine aquaporins: gating of a tonoplast intrinsic protein (TIP2;1) by cytosolic pH. *PLOS ONE* 7:e33219
114. Li GW, Tillard P, Gojon A, Maurel C. 2016. Dual regulation of root hydraulic conductivity and plasma membrane aquaporins by plant nitrate accumulation and high-affinity nitrate transporter NRT2.1. *Plant Cell Physiol.* 57:733–42
115. Li L, Wang H, Gago J, Cui HY, Qian ZJ, et al. 2015. Harpin Hpa1 interacts with aquaporin PIP1;4 to promote the substrate transport and photosynthesis in Arabidopsis. *Sci. Rep.* 5:17207
116. Li P, Zhang LY, Mo XY, Ji HT, Bian HJ, et al. 2019. Rice aquaporin PIP1;3 and harpin Hpa1 of bacterial blight pathogen cooperate in a type III effector translocation. *J. Exp. Bot.* 70:3057–73
117. Li X, Wang X, Yang Y, Li R, He Q, et al. 2011. Single-molecule analysis of PIP2;1 dynamics and partitioning reveals multiple modes of *Arabidopsis* plasma membrane aquaporin regulation. *Plant Cell* 23:3780–97
118. Lian HL, Yu X, Lane D, Sun WN, Tang ZC, Su WA. 2006. Upland rice and lowland rice exhibited different *PIP* expression under water deficit and ABA treatment. *Cell Res.* 16:651–60
119. Lian HL, Yu X, Ye Q, Ding XS, Kitagawa Y, et al. 2004. The role of aquaporin RWC3 in drought avoidance in rice. *Plant Cell Physiol.* 45:481–89
120. Lindahl V, Gourdon P, Andersson M, Hess B. 2018. Permeability and ammonia selectivity in aquaporin TIP2;1: linking structure to function. *Sci. Rep.* 8:2995
121. Liu K, Kozono D, Kato Y, Agre P, Hazama A, Yasui M. 2005. Conversion of aquaporin 6 from an anion channel to a water-selective channel by a single amino acid substitution. *PNAS* 102:2192–97
122. Liu LH, Ludewig U, Gassert B, Frommer WB, von Wiren N. 2003. Urea transport by nitrogen-regulated tonoplast intrinsic proteins in Arabidopsis. *Plant Physiol.* 133:1220–28
123. Liu SY, Fukumoto T, Gena P, Feng P, Sun Q, et al. 2020. Ectopic expression of a rice plasma membrane intrinsic protein (OsPIP1;3) promotes plant growth and water uptake. *Plant J.* 102:779–96
124. Loque D, Ludewig U, Yuan LX, von Wiren N. 2005. Tonoplast intrinsic proteins AtTIP2;1 and AtTIP2;3 facilitate NH<sub>3</sub> transport into the vacuole. *Plant Physiol.* 137:671–80
125. MacRobbie EAC. 2006. Osmotic effects on vacuolar ion release in guard cells. *PNAS* 103:1135–40
126. MacRobbie EAC, Smyth WD. 2010. Effects of fusicoccin on ion fluxes in guard cells. *New Phytol.* 186:636–47
127. Martinière A, Fiche JB, Smokvarska M, Mari S, Alcon C, et al. 2019. Osmotic stress activates two reactive oxygen species pathways with distinct effects on protein nanodomains and diffusion. *Plant Physiol.* 179:1581–93
128. Masalkar P, Wallace IS, Hwang JH, Roberts DM. 2010. Interaction of cytosolic glutamine synthetase of soybean root nodules with the C-terminal domain of the symbiosome membrane nodulin 26 aquaglyceroporin. *J. Biol. Chem.* 285:23880–88
129. Matsumoto T, Lian HL, Su WA, Tanaka D, Liu CW, et al. 2009. Role of the aquaporin PIP1 subfamily in the chilling tolerance of rice. *Plant Cell Physiol.* 50:216–29
130. Maurel C, Boursiac Y, Luu DT, Santoni V, Shahzad Z, Verdoucq L. 2015. Aquaporins in plants. *Physiol. Rev.* 95:1321–58
131. Maurel C, Reizer J, Schroeder JI, Chrispeels MJ. 1993. The vacuolar membrane protein  $\gamma$ -TIP creates water specific channels in *Xenopus* oocytes. *EMBO J.* 12:2241–47
132. McGaughey SA, Qiu J, Tyerman SD, Byrt CS. 2018. Regulating root aquaporin function in response to changes in salinity. *Annu. Plant Rev. Online.* <http://doi.org/10.1002/9781119312994.apr0626>

---

123. Shows that OsPIP1;3 elicited an anion conductance to NO<sub>3</sub><sup>-</sup> but not HCO<sub>3</sub><sup>-</sup>/CO<sub>3</sub><sup>2-</sup> when expressed in HEK293 cells.

---

133. McLoughlin F, Arisz SA, Dekker HL, Kramer G, de Koster CG, et al. 2013. Identification of novel candidate phosphatidic acid-binding proteins involved in the salt-stress response of *Arabidopsis thaliana* roots. *Biochem. J.* 450:573–81
134. Munns R, Day DA, Fricke W, Watt M, Arsova B, et al. 2020. Energy costs of salt tolerance in crop plants. *New Phytol.* 225:1072–90
135. Nguyen MX, Moon S, Jung KH. 2013. Genome-wide expression analysis of rice aquaporin genes and development of a functional gene network mediated by aquaporin expression in roots. *Planta* 238:669–81
136. Niemietz CM, Tyerman SD. 2000. Channel-mediated permeation of ammonia gas through the peribacteroid membrane of soybean nodules. *FEBS Lett.* 465:110–14
137. Noronha H, Araujo D, Conde C, Martins AP, Soveral G, et al. 2016. The grapevine uncharacterized intrinsic protein 1 (VvXIP1) is regulated by drought stress and transports glycerol, hydrogen peroxide, heavy metals but not water. *PLOS ONE* 11:e0160976
138. Nyblom M, Frick A, Wang Y, Ekwall M, Hallgren K, et al. 2009. Structural and functional analysis of SoPIP2;1 mutants adds insight into plant aquaporin gating. *J. Mol. Biol.* 387:653–68
139. Obermeyer G, Tyerman SD. 2005. NH<sub>4</sub><sup>+</sup> currents across the peribacteroid membrane of soybean. Macroscopic and microscopic properties, inhibition by Mg<sup>2+</sup>, and temperature dependence indicate a subpicoSiemens channel finely regulated by divalent cations. *Plant Physiol.* 139:1015–29
140. Otto B, Uehlein N, Sdorra S, Fischer M, Ayaz M, et al. 2010. Aquaporin tetramer composition modifies the function of tobacco aquaporins. *J. Biol. Chem.* 285:31253–60
141. Ouyang L-J, Whelan J, Weaver CD, Roberts DM, Day DA. 1991. Protein phosphorylation stimulates the rate of malate uptake across the peribacteroid membrane of soybean nodules. *FEBS Lett.* 293:188–90
142. Ozu M, Dorr RA, Gutierrez F, Politi MT, Toriano R. 2013. Human AQP1 is a constitutively open channel that closes by a membrane-tension-mediated mechanism. *Biophys. J.* 104:85–95
143. Pei JV, Heng S, De Ieso ML, Sylvia GM, Kourghi M, et al. 2019. Lithium ‘hot-spots’: real-time analysis of non-selective cation channel activity in migrating cancer cells. *Mol. Pharmacol.* 95:573–83
144. Peiter E, Maathuis FJM, Mills LN, Knight H, Pelloux J, et al. 2005. The vacuolar Ca<sup>2+</sup>-activated channel TPC1 regulates germination and stomatal movement. *Nature* 434:404–8
145. Pellegrini-Calace M, Maiwald T, Thornton JM. 2009. PoreWalker: a novel tool for the identification and characterization of channels in transmembrane proteins from their three-dimensional structure. *PLOS Comput. Biol.* 5:e10000440
146. Péret B, Li GW, Zhao J, Band LR, Voß U, et al. 2012. Auxin regulates aquaporin function to facilitate lateral root emergence. *Nat. Cell Biol.* 14:991–98
147. Pommerrenig B, Diehn TA, Bernhardt N, Bienert MD, Mitani-Ueno N, et al. 2020. Functional evolution of nodulin 26-like intrinsic proteins: from bacterial arsenic detoxification to plant nutrient transport. *New Phytol.* 225:1383–96
148. Pommerrenig B, Diehn TA, Bienert GP. 2015. Metalloido-porins: essentiality of Nodulin 26-like intrinsic proteins in metalloid transport. *Plant Sci.* 238:212–27
149. Pottosin II, Martinez-Estevéz M. 2003. Regulation of the fast vacuolar channel by cytosolic and vacuolar potassium. *Biophys. J.* 84:977–86
150. Pou A, Medrano H, Flexas J, Tyerman SD. 2013. A putative role for TIP and PIP aquaporins in dynamics of leaf hydraulic and stomatal conductances in grapevine under water stress and re-watering. *Plant Cell Environ.* 36:828–43
151. Prado K, Boursiac Y, Tournaire-Roux C, Monneuse JM, Postaire O, et al. 2013. Regulation of *Arabidopsis* leaf hydraulics involves light-dependent phosphorylation of aquaporins in veins. *Plant Cell* 25:1029–39
152. Prado K, Cotellet V, Li G, Bellati J, Tang N, et al. 2019. Oscillating aquaporin phosphorylation and 14-3-3 proteins mediate the circadian regulation of leaf hydraulics. *Plant Cell* 31:417–29
153. **Prak S, Hem S, Boudet J, Viennois G, Sommerer N, et al. 2008. Multiple phosphorylations in the C-terminal tail of plant plasma membrane aquaporins: Role in subcellular trafficking of AtPIP2;1 in response to salt stress. *Mol. Cell. Proteom.* 7:1019–30**
154. Pravda L, Sehnal D, Toušek D, Navrátilová V, Bazgier V, et al. 2018. MOLEonline: a web-based tool for analyzing channels, tunnels and pores (2018 update). *Nucleic Acids Res.* 46:W368–73
155. Preston GM, Carroll TP, Guggino WB, Agre P. 1992. Appearance of water channels in *Xenopus* oocytes expressing red-cell CHIP28 protein. *Science* 256:385–87

---

153. Shows that AtPIP2;1 C-terminal site phosphorylation was affected by salinity and H<sub>2</sub>O<sub>2</sub> and influenced intracellular AtPIP2;1 accumulation.

---

156. Qin X, Boron WF. 2013. Mutation of a single amino acid converts the human water channel aquaporin 5 into an anion channel. *Am. J. Physiol. Cell Physiol.* 305:C663–72
157. Qing D, Yang Z, Li M, Wong WS, Guo G, et al. 2016. Quantitative and functional phosphoproteomic analysis reveals that ethylene regulates water transport via the C-terminal phosphorylation of aquaporin PIP2;1 in *Arabidopsis*. *Mol. Plant* 9(1):158–74
158. Qiu J, McGaughey SA, Groszmann M, Tyerman SD, Byrt CS. 2020. Phosphorylation influences water and ion channel function of AtPIP2;1. *Plant Cell Environ.* 43:2428–42
159. Rao SL, Lynch CI, Klesse G, Oakley GE, Stansfeld PJ, et al. 2018. Water and hydrophobic gates in ion channels and nanopores. *Faraday Discuss.* 209:231–47
160. Raven JA, Doblin MA. 2014. Active water transport in unicellular algae: where, why, and how. *J. Exp. Bot.* 65:6279–92
161. Regan JW, Stamer WD, Yool AJ. 1997. Aquaporins and ion conductance. *Science* 275:1490–92
162. Reichel M, Liao Y, Rettel M, Ragan C, Evers M, et al. 2016. In planta determination of the mRNA-binding proteome of *Arabidopsis* etiolated seedlings. *Plant Cell* 28:2435–52
163. Reinhardt H, Hachez C, Bienert MD, Beebo A, Swarup K, et al. 2016. Tonoplast aquaporins facilitate lateral root emergence. *Plant Physiol.* 170:1640–54
164. Rigo E, Dong Z, Park JH, Kennedy E, Hokmabadi M, et al. 2019. Measurements of the size and correlations between ions using an electrolytic point contact. *Nat. Commun.* 10:2382
165. Rivers RL, Dean RM, Chandry G, Hall JE, Roberts DM, Zeidel ML. 1997. Functional analysis of nodulin 26, an aquaporin in soybean root nodule symbiosomes. *J. Biol. Chem.* 272:16256–61
166. Roberts DM, Tyerman SD. 2002. Voltage-dependent cation channels permeable to  $\text{NH}_4^+$ ,  $\text{K}^+$ , and  $\text{Ca}^{2+}$  in the symbiosome membrane of the model legume *Lotus japonicus*. *Plant Physiol.* 128:370–78
167. Rodrigues O, Reshetnyak G, Grondin A, Saijo Y, Leonhardt N, et al. 2017. Aquaporins facilitate hydrogen peroxide entry into guard cells to mediate ABA- and pathogen-triggered stomatal closure. *PNAS* 114:9200–5
168. Rubio F, Flores P, Navarro JM, Martínez V. 2003. Effects of  $\text{Ca}^{2+}$ ,  $\text{K}^+$  and cGMP on  $\text{Na}^+$  uptake in pepper plants. *Plant Sci.* 165:1043–49
169. Sade N, Weng F, Tajima H, Zeron Y, Zhang L, et al. 2020. A cytoplasmic receptor-like kinase contributes to salinity tolerance. *Plants* 9(10):1383
170. Sahr T, Adam T, Fizames C, Maurel C, Santoni V. 2010. *O*-carboxyl- and *N*-methyltransferases active on plant aquaporins. *Plant Cell Physiol.* 51:2092–104
171. Sakr S, Alves G, Morillon RL, Maurel K, Decourteix M, et al. 2003. Plasma membrane aquaporins are involved in winter embolism recovery in walnut tree. *Plant Physiol.* 133:630–41
172. Sakurai J, Ishikawa F, Yamaguchi T, Uemura M, Maeshima M. 2005. Identification of 33 rice aquaporin genes and analysis of their expression and function. *Plant Cell Physiol.* 46:1568–77
173. Sansom MSP, Weinstein H. 2000. Hinges, swivels and switches: the role of prolines in signalling via transmembrane alpha-helices. *Trends Pharmacol. Sci.* 21:445–51
174. Santoni V, Verdoucq L, Sommerer N, Vinh J, Pflieger D, Maurel C. 2006. Methylation of aquaporins in plant plasma membrane. *Biochem. J.* 400:189–97
175. Saparov SM, Kozono D, Rothe U, Agre P, Pohl P. 2001. Water and ion permeation of aquaporin-1 in planar lipid bilayers. Major differences in structural determinants and stoichiometry. *J. Biol. Chem.* 276:31515–20
176. Saparov SM, Liu K, Agre P, Pohl P. 2007. Fast and selective ammonia transport by aquaporin-8. *J. Biol. Chem.* 282:5296–301
177. Sassi A, Mieulet D, Khan I, Moreau B, Gaillard I, et al. 2012. The rice monovalent cation transporter OsHKT2;4: revisited ionic selectivity. *Plant Physiol.* 160:498–510
178. Savage DF, Egea PF, Robles-Colmenares Y, O'Connell JD, Stroud RM. 2003. Architecture and selectivity in aquaporins: 2.5 angstrom X-ray structure of aquaporin Z. *PLOS Biol.* 1:334–40
179. Schuurmans J, van Dongen JT, Rutjens BPW, Boonman A, Pieterse CMJ, Borstlap AC. 2003. Members of the aquaporin family in the developing pea seed coat include representatives of the PIP, TIP, and NIP subfamilies. *Plant Mol. Biol.* 53:655–67
180. Secchi F, Pagliarani C, Zwieniecki MA. 2017. The functional role of xylem parenchyma cells and aquaporins during recovery from severe water stress. *Plant Cell Environ.* 40:858–71

---

188. Explains the structure of spinach SoPIP2;l (open and closed), showing how Loop D functions as a gate.

---

190. Shows that HvPIP2;8 is an iCAQP permeable to Na<sup>+</sup> and K<sup>+</sup> but not Rb<sup>+</sup>, Cs<sup>+</sup>, or Li<sup>+</sup>.

---

181. Sjövall-Larsen S, Alexandersson E, Johansson I, Karlsson M, Johanson U, Kjellbom P. 2006. Purification and characterization of two protein kinases acting on the aquaporin SoPIP2;1. *Biochim. Biophys. Acta Biomembr.* 1758:1157–64
182. Skerrett M, Tyerman SD. 1994. A channel that allows inwardly directed fluxes of anions in protoplasts derived from wheat roots. *Planta* 192:295–305
183. Sobczak K, Bangel-Ruland N, Leier G, Weber WM. 2010. Endogenous transport systems in the *Xenopus laevis* oocyte plasma membrane. *Methods* 51:183–89
184. Sui HX, Han BG, Lee JK, Walian P, Jap BK. 2001. Structural basis of water-specific transport through the AQP1 water channel. *Nature* 414:872–78
185. Teakle NL, Tyerman SD. 2010. Mechanisms of Cl<sup>-</sup> transport contributing to salt tolerance. *Plant Cell Environ.* 33:566–89
186. Temmei Y, Uchida S, Hoshino D, Kanzawa N, Kuwahara M, et al. 2005. Water channel activities of *Mimosa pudica* plasma membrane intrinsic proteins are regulated by direct interaction and phosphorylation. *FEBS Lett.* 579:4417–22
187. Tikhonova LI, Pottosin II, Dietz KJ, Schönknecht G. 1997. Fast-activating cation channel in barley mesophyll vacuoles. Inhibition by calcium. *Plant J.* 11:1059–70
188. **Törnroth-Horsefield S, Wang Y, Hedfalk K, Johanson U, Karlsson M, et al. 2006. Structural mechanism of plant aquaporin gating. *Nature* 439:688–94**
189. Tournaire-Roux C, Sutka M, Javot H, Gout E, Gerbeau P, et al. 2003. Cytosolic pH regulates root water transport during anoxic stress through gating of aquaporins. *Nature* 425:393–97
190. **Tran STH, Imran S, Horie T, Qiu J, McGaughy S, et al. 2020. A survey of barley PIP aquaporin ionic conductance reveals Ca<sup>2+</sup>-sensitive HvPIP2;8 Na<sup>+</sup> and K<sup>+</sup> conductance. *Int. J. Mol. Sci.* 21:7135**
191. Tsunoda SP, Wiesner B, Lorenz D, Rosenthal W, Pohl P. 2004. Aquaporin-1, nothing but a water channel. *J. Biol. Chem.* 279:11364–67
192. Tyerman SD, Skerrett M, Garrill A, Findlay GP, Leigh RA. 1997. Pathways for the permeation of Na<sup>+</sup> and Cl<sup>-</sup> into protoplasts derived from the cortex of wheat roots. *J. Exp. Bot.* 48:459–80
193. Tyerman SD, Whitehead LF, Day DA. 1995. A channel-like transporter for NH<sub>4</sub><sup>+</sup> on the symbiotic interface of N<sub>2</sub>-fixing plants. *Nature* 378:629–32
194. Tyerman SD, Wignes JA, Kaiser BN. 2017. Root hydraulic and aquaporin responses to N availability. In *Plant Aquaporins: Signaling and Communication in Plants*, ed. F Chaumont, SD Tyerman, pp. 207–36. Cham, Switz.: Springer
195. Tzounopoulos T, Maylie J, Adelman JP. 1995. Induction of endogenous channels by high levels of heterologous membrane-proteins in *Xenopus* oocytes. *Biophys. J.* 69:904–8
196. Ueda M, Tsutsumi N, Fujimoto M. 2016. Salt stress induces internalization of plasma membrane aquaporin into the vacuole in *Arabidopsis thaliana*. *Biochem. Biophys. Res. Commun.* 474:742–46
197. Uehlein N, Lovisolo C, Siefritz F, Kaldenhoff R. 2003. The tobacco aquaporin NtAQP1 is a membrane CO<sub>2</sub> pore with physiological functions. *Nature* 425:734–37
198. Van Wilder V, Micielica U, Degand H, Derua R, Waelkens E, Chaumont F. 2008. Maize plasma membrane aquaporins belonging to the PIP1 and PIP2 subgroups are in vivo phosphorylated. *Plant Cell Physiol.* 49:1364–77
199. Vandeleur R, Niemietz C, Tilbrook J, Tyerman SD. 2005. Roles of aquaporins in root responses to irrigation. *Plant Soil* 274:141–61
200. Verdoucq L, Grondin A, Maurel C. 2008. Structure–function analysis of plant aquaporin AtPIP2;1 gating by divalent cations and protons. *Biochem. J.* 415:409–16
201. Verdoucq L, Maurel C. 2018. Plant aquaporins. *Advanc. Bot. Res.* 87:25–56
202. Vitali V, Jozefkowicz C, Fortuna AC, Soto G, Flecha FLG, Allewa K. 2019. Cooperativity in proton sensing by PIP aquaporins. *FEBS J.* 286:991–1002
203. Wallace IS, Roberts DM. 2004. Homology modeling of representative subfamilies of Arabidopsis major intrinsic proteins. Classification based on the aromatic/arginine selectivity filter. *Plant Physiol.* 135:1059–68
204. Wan XC, Steudle E, Hartung W. 2004. Gating of water channels (aquaporins) in cortical cells of young corn roots by mechanical stimuli (pressure pulses): effects of ABA and of HgCl<sub>2</sub>. *J. Exp. Bot.* 55:411–22

205. Wang C, Hu H, Qin X, Zeise B, Xu D, et al. 2015. Reconstitution of CO<sub>2</sub> regulation of SLAC1 anion channel and function of CO<sub>2</sub>-permeable PIP2;1 aquaporin as CARBONIC ANHYDRASE4 interactor. *Plant Cell* 28:568–82
206. Wang H, Schoebel S, Schmitz F, Dong H, Hedfalk K. 2020. Characterization of aquaporin-driven hydrogen peroxide transport. *Biochim. Biophys. Acta Biomembr.* 1862:183065
207. Wang Y, Tajkhorshid E. 2010. Nitric oxide conduction by the brain aquaporin AQP4. *Proteins* 78:661–70
208. Wang YQ, Li RH, Li DM, Jia XM, Zhou DW, et al. 2017. NIP1;2 is a plasma membrane-localized transporter mediating aluminum uptake, translocation, and tolerance in *Arabidopsis*. *PNAS* 114:5047–52
209. Watanabe S, Moniaga CS, Nielsen S, Hara-Chikuma M. 2016. Aquaporin-9 facilitates membrane transport of hydrogen peroxide in mammalian cells. *Biochem. Biophys. Res. Commun.* 471:191–97
210. Weaver CD, Shomer NH, Louis CF, Roberts DM. 1994. Nodulin 26, a nodule-specific symbiosome membrane protein from soybean, is an ion channel. *J. Biol. Chem.* 269:17858–62
211. Wegner LH. 2014. Root pressure and beyond: energetically uphill water transport into xylem vessels? *J. Exp. Bot.* 65:381–93
212. Wegner LH. 2015. A thermodynamic analysis of the feasibility of water secretion into xylem vessels against a water potential gradient. *Funct. Plant Biol.* 42:828–35
213. Wegner LH. 2017. Cotransport of water and solutes in plant membranes: the molecular basis, and physiological functions. *AIMS Biophys.* 4:192–209
214. Wienkoop S, Saalbach G. 2003. Proteome analysis. Novel proteins identified at the peribacteroid membrane from *Lotus japonicus* root nodules. *Plant Physiol.* 131:1080–90
215. Wree D, Wu BH, Zeuthen T, Beitz E. 2011. Requirement for asparagine in the aquaporin NPA sequence signature motifs for cation exclusion. *FEBS J.* 278:740–48
216. Wu BH, Steinbronn C, Alsterfjord M, Zeuthen T, Beitz E. 2009. Concerted action of two cation filters in the aquaporin water channel. *EMBO J.* 28:2188–94
217. Wu FQ, Sheng PK, Tan JJ, Chen XL, Lu GW, et al. 2015. Plasma membrane receptor-like kinase leaf panicle 2 acts downstream of the DROUGHT AND SALT TOLERANCE transcription factor to regulate drought sensitivity in rice. *J. Exp. Bot.* 66:271–81
218. Wu XN, Rodriguez CS, Pertl-Obermeyer H, Obermeyer G, Schulze WX. 2013. Sucrose-induced receptor kinase SIRK1 regulates a plasma membrane aquaporin in *Arabidopsis*. *Mol. Cell. Proteom.* 12:2856–73
219. Wudick MM, Li X, Valentini V, Geldner N, Chory J, et al. 2015. Subcellular redistribution of root aquaporins induced by hydrogen peroxide. *Mol. Plant* 8:1103–14
220. Wudick MM, Luu DT, Maurel C. 2009. A look inside: localization patterns and functions of intracellular plant aquaporins. *New Phytol.* 184:289–302
221. Yaneff A, Sigaut L, Gómez N, Aliaga Fandiño C, Alleva K, et al. 2016. Loop B serine of a plasma membrane aquaporin type PIP2 but not PIP1 plays a key role in pH sensing. *Biochim. Biophys. Acta Biomembr.* 1858:2778–87
222. Yaneff A, Sigaut L, Marquez M, Alleva K, Pietrasanta LI, Amodeo G. 2014. Heteromerization of PIP aquaporins affects their intrinsic permeability. *PNAS* 111:231–36
223. Yaneff A, Vitali V, Amodeo G. 2015. PIP1 aquaporins: intrinsic water channels or PIP2 aquaporin modulators? *FEBS Lett.* 589:3508–15
224. Yang O, Popova OV, Suthoff U, Luking I, Dietz KJ, Golldack D. 2009. The *Arabidopsis* basic leucine zipper transcription factor *AtbZIP24* regulates complex transcriptional networks involved in abiotic stress resistance. *Gene* 436:45–55
225. Yasui M. 2009. pH regulated anion permeability of aquaporin-6. *Handb. Exp. Pharmacol.* 190:299–308
226. Yasui M, Hazama A, Kwon TH, Nielsen S, Guggino WB, Agre P. 1999. Rapid gating and anion permeability of an intracellular aquaporin. *Nature* 402:184–87
227. Ye Q, Muhr J, Steudle E. 2005. A cohesion/tension model for the gating of aquaporins allows estimation of water channel pore volumes in *Chara*. *Plant Cell Environ.* 28:525–35
228. Yoo YJ, Lee HK, Han W, Kim DH, Lee MH, et al. 2016. Interactions between transmembrane helices within monomers of the aquaporin AtPIP2;1 play a crucial role in tetramer formation. *Mol. Plant* 9:1004–17
229. Yool AJ, Campbell EM. 2012. Structure, function and translational relevance of aquaporin dual water and ion channels. *Mol. Asp. Med.* 33:553–61

---

205. Explains that AtPIP2;1 with a carbonic anhydrase in *Xenopus* oocytes enables SLAC1 anion channel sensitivity to CO<sub>2</sub>.

---

---

236. Shows that drought triggers phosphorylation of RhPIP2;1 and nuclear translocation of the interacting membrane-bound transcription factor, slowing growth.

---

230. Yool AJ, Stamer WD, Regan JW. 1996. Forskolin stimulation of water and cation permeability in aquaporin 1 water channels. *Science* 273:1216–18
231. Yool AJ, Weinstein AM. 2002. New roles for old holes: ion channel function in aquaporin-1. *News Physiol. Sci.* 17:68–72
232. Yu J, Yool AJ, Schulten K, Tajkhorshid E. 2006. Mechanism of gating and ion conductivity of a possible tetrameric pore in aquaporin-1. *Structure* 14:1411–23
233. Zelazny E, Borst JW, Muylaert M, Batoko H, Hemminga MA, Chaumont F. 2007. FRET imaging in living maize cells reveals that plasma membrane aquaporins interact to regulate their subcellular localization. *PNAS* 104:12359–64
234. Zeuthen T, MacAulay N. 2012. Cotransport of water by  $\text{Na}^+ - \text{K}^+ - 2\text{Cl}^-$  cotransporters expressed in *Xenopus* oocytes: NKCC1 versus NKCC2. *J. Physiol.* 590:1139–54
235. Zhang MH, Lu SQ, Li GW, Mao ZL, Yu X, et al. 2010. Identification of a residue in helix 2 of rice plasma membrane intrinsic proteins that influences water permeability. *J. Biol. Chem.* 285:41982–92
236. **Zhang S, Feng M, Chen W, Zhou XF, Lu JY, et al. 2019. In rose, transcription factor PTM balances growth and drought survival via PIP2;1 aquaporin. *Nat. Plants* 5:290–99**
237. Zhang W, Zitron E, Hö M, Kihm L, Morath C, et al. 2007. Aquaporin-1 channel function is positively regulated by protein kinase C. *J. Biol. Chem.* 282:20933–40
238. Zhang Y, McBride DW, Hamill OP. 1998. The ion selectivity of a membrane conductance inactivated by extracellular calcium in *Xenopus* oocytes. *J. Physiol.* 508:763–76
239. Zhu DL, Wu Z, Cao GY, Li JG, Wei J, et al. 2014. TRANSLUCENT GREEN, an ERF family transcription factor, controls water balance in *Arabidopsis* by activating the expression of aquaporin genes. *Mol. Plant* 7:601–15
240. Zwiazek JJ, Xu H, Tan X, Navarro-Ródenas A, Morte A, et al. 2017. Significance of oxygen transport through aquaporins. *Sci. Rep.* 7:40411